

AD\_\_\_\_\_

Award Number: W81XWH-09-2-0067

TITLE: Determining the Marker Configuration and Modeling Technique to Optimize the Biomechanical Analysis of Running-Specific Prostheses

PRINCIPAL INVESTIGATOR: Jae Kun Shim, Ph.D.

CONTRACTING ORGANIZATION: University of Maryland, College Park  
College Park, MD 20742-5100

REPORT DATE: March 2012

TYPE OF REPORT: Final

PREPARED FOR: U.S. Army Medical Research and Materiel Command  
Fort Detrick, Maryland 21702-5012

DISTRIBUTION STATEMENT: Approved for Public Release;  
Distribution Unlimited

The views, opinions and/or findings contained in this report are those of the author(s) and should not be construed as an official Department of the Army position, policy or decision unless so designated by other documentation.

<b>REPORT DOCUMENTATION PAGE</b>			<i>Form Approved</i> <i>OMB No. 0704-0188</i>		
Public reporting burden for this collection of information is estimated to average 1 hour per response, including the time for reviewing instructions, searching existing data sources, gathering and maintaining the data needed, and completing and reviewing this collection of information. Send comments regarding this burden estimate or any other aspect of this collection of information, including suggestions for reducing this burden to Department of Defense, Washington Headquarters Services, Directorate for Information Operations and Reports (0704-0188), 1215 Jefferson Davis Highway, Suite 1204, Arlington, VA 22202-4302. Respondents should be aware that notwithstanding any other provision of law, no person shall be subject to any penalty for failing to comply with a collection of information if it does not display a currently valid OMB control number. <b>PLEASE DO NOT RETURN YOUR FORM TO THE ABOVE ADDRESS.</b>					
<b>1. REPORT DATE</b> March 2012		<b>2. REPORT TYPE</b> Final		<b>3. DATES COVERED</b> 1 August 2009 – 31 Dec 2012	
<b>4. TITLE AND SUBTITLE</b>  Determining the Marker Configuration and Modeling Technique to Optimize the Biomechanical Analysis of Running-Specific Prostheses			<b>5a. CONTRACT NUMBER</b>		
			<b>5b. GRANT NUMBER</b> W81XWH-09-2-0067		
			<b>5c. PROGRAM ELEMENT NUMBER</b>		
<b>6. AUTHOR(S)</b>  Jae Kun Shim, Ph.D. Adam Hsieh, Ph.D.; Alison Linberg, DPT; Erik Wolf, Ph.D.  <b>E-Mail:</b> jkshim@umd.edu			<b>5d. PROJECT NUMBER</b>		
			<b>5e. TASK NUMBER</b>		
			<b>5f. WORK UNIT NUMBER</b>		
<b>7. PERFORMING ORGANIZATION NAME(S) AND ADDRESS(ES)</b>  University of Maryland, College Park College Park, MD 20742-5100			<b>8. PERFORMING ORGANIZATION REPORT NUMBER</b>		
<b>9. SPONSORING / MONITORING AGENCY NAME(S) AND ADDRESS(ES)</b> U.S. Army Medical Research and Materiel Command Fort Detrick, Maryland 21702-5012			<b>10. SPONSOR/MONITOR'S ACRONYM(S)</b>		
			<b>11. SPONSOR/MONITOR'S REPORT NUMBER(S)</b>		
<b>12. DISTRIBUTION / AVAILABILITY STATEMENT</b> Approved for Public Release; Distribution Unlimited					
<b>13. SUPPLEMENTARY NOTES</b>					
<b>14. ABSTRACT</b>  The purpose of this study was to develop and validate a model with optimal set-up of reflective markers, producing minimal errors in inverse dynamics calculations. The Statement of Work for this project indicated two specific aims. Specific Aim 1 proposed to develop and validate a model with unique optimal marker placements for specific running prosthesis designs. The proposed timeline indicated that preparation for the experimental setting and formulation of the program for data analysis would occur during Months 1-8. These milestones were reached on schedule. During Months 8-16, we proposed to complete MTS testing, begin validating the general model, and begin analyzing the MTS data to determine the final marker model for each running-specific prosthesis. Some of these milestones were delayed due to procurement issues arising from the prosthesis manufacturers. A no-cost extension until 28 February 2012 was granted due to these issues. These milestones were completed as anticipated upon prosthesis procurement. The results of this study indicate that marker placement and number of markers on a running-specific prosthesis did not greatly influence the accuracy of kinetic data of the running prosthesis designs tested. A draft of a manuscript detailing the study results is included as an Appendix to this report.					
<b>15. SUBJECT TERMS</b> Force, Moment, Inverse Dynamics, Biomechanics, Model, Running, Prosthesis					
<b>16. SECURITY CLASSIFICATION OF:</b>			<b>17. LIMITATION OF ABSTRACT</b>	<b>18. NUMBER OF PAGES</b>	<b>19a. NAME OF RESPONSIBLE PERSON</b> USAMRMC
<b>a. REPORT</b> U	<b>b. ABSTRACT</b> U	<b>c. THIS PAGE</b> U			<b>19b. TELEPHONE NUMBER</b> (include area code)
			UU	71	

## Table of Contents

	<u>Page</u>
<b>Introduction</b> .....	<b>4</b>
<b>Body</b> .....	<b>5</b>
<b>Key Research Accomplishments</b> .....	<b>14</b>
<b>Reportable Outcomes</b> .....	<b>15</b>
<b>Conclusions</b> .....	<b>16</b>
<b>References</b> .....	<b>17</b>
<b>Appendix I: Personnel Receiving Pay</b> .....	<b>19</b>
<b>Appendix II: Manuscript Draft 1</b> .....	<b>20</b>
<i>Marker Placement on Running-Specific Prostheses Does Not Affect Kinetics</i>	
<b>Appendix III: Manuscript Draft 2</b> .....	<b>46</b>
<i>Determining the Inertial Properties of Running-Specific Prostheses</i>	

## Introduction

While running has been shown to reduce disease risks and promote a generally healthy lifestyle in uninjured people, very little running-specific research is available pertaining to the amputee population. The little existing amputee running literature primarily involves running with prostheses designed for every day wear, which are typically prescribed and aligned to perform optimally during standing and walking. Further, these studies have used biomechanical models designed for the intact limb to estimate joint kinetics (forces and moments) using an inverse dynamics approach. This approach estimates distal joint kinetics and uses these calculations to estimate more proximal joint kinetics. Consequently, inverse dynamics estimations rely on accurate estimation of the ankle joint as errors will be propagated and inflated with more proximal calculations. The previous studies on amputee running have not validated the methodology used for joint kinetic measurements with running-specific prostheses, which can potentially prove to be erroneous.<sup>1-3</sup> These limitations call for systematic research and development of validated models for running-specific prostheses. This will lead to improved prosthetic designs that will allow clinicians to provide evidence-based exercise prescriptions to amputees, enabling them to comfortably and efficiently run. The objective of the proposed study is to develop and validate a model with optimal set-up of reflective markers used in 3D gait analysis, producing minimal errors in inverse dynamics calculations. The long-term objective of this project is to understand the biomechanical and physiological consequences of amputation, to develop an optimal design of activity-independent lower-extremity prosthesis, and to help clinicians prescribing appropriate prosthesis and exercise regimes to people with a lower extremity amputation.

Please see *Appendix II: Manuscript Draft 1* for a more detailed introduction.

The current project was approved for funding over 18 months beginning 1 August, 2009 and to be completed by 28 February, 2011. A no-cost extension was approved due to issues in prosthesis procurement caused by the prosthetic manufacturing companies. The extension was approved through 28 February, 2012.

The purpose of this document is to provide details of the study to satisfy the Final Report requirement.

## Body

The approved Statement of Work proposed the following timeline (Table 1):

**Table 1.** Timeline for approved project.

	Months 1-6	Months 7-12	Months 13-18
Specific Aim #1: Development and validation of a model with unique optimal marker placements for specific running prosthesis designs			
Formulate program for data analysis	X		
MTS testing of running specific prostheses (12 prostheses)	X		
Validation of model		X	
Analysis of MTS data to determine model		X	
Specific Aim #2: Determination of the resultant optimal marker placement for all tested running prosthetic designs			
Determine model with optimal marker placement for across designs			X

### Methodology

A biomechanical model was developed using motion analysis of running-specific prostheses in a material testing system (MTS, Eden Prairie, MN). Four running-specific prosthesis designs (Figure 1) were tested for this project including the 1E90 Sprinter (OttoBock Inc.), Flex-Run (Ossur), Cheetah<sup>®</sup> (Ossur) and Nitro Running Foot (Freedom Innovations). These prostheses were chosen because they are the most commonly prescribed running-specific prostheses currently available on the market. Three different stiffness categories were also tested for each prosthetic design to identify whether prosthetic stiffness affects optimal marker placement. Stiffness categories were chosen to reflect a common range of stiffnesses that might be prescribed.

Each prosthesis was placed in the MTS between two load cells (Bertec PY6, Columbus, OH) in a neutral alignment. Neutral alignment was defined according to the specific manufacturers' recommendations for prosthesis alignment. The load cells captured data at 1,000 Hz. The prostheses were cyclically loaded for ten cycles with axial forces up to 2,500 N to simulate peak vertical forces commonly observed during running (approximately three times the body weight of a 75 kg person). The load cells measured the force and moment at the point of load application proximal to the prostheses (applied load) and the reaction forces distal to the prostheses (ground reaction forces).

Reflective markers were placed at 2 cm intervals along the lateral aspect of the keel of each running-specific prosthesis (Figure 2). Reflective markers were also placed orthogonally on the anterior, lateral, and medial aspect of the "head" of the prosthesis, at the point of connection to the socket or pylon, in order to define the local coordinate system of the prosthesis. Three additional markers were placed along the midline of each prosthesis to define a plane to which the keel markers were projected for further analysis. An 8-camera motion capture system (Vicon, Oxford, UK) with a capture frequency of 500 Hz was used to collect the 3-D positional data of the markers during each trial. Two consecutive projected center line markers defined individual segments of the prosthesis (assumed to be rigid) and consecutive segments shared a common marker. The joint between these segments was assumed as a hinge joint. Standard inverse dynamics calculations (equations 1 and 2) were used to estimate the force and torque transfer from the ground reaction force, through the defined prosthesis segments, and to the point of load application proximal to the prosthesis.



**Figure 1.** Prostheses used for mechanical testing.

$$F_i - F_{i+1} + m_i g = m_i a_i \quad [1]$$

$$M_i - M_{i+1} + r_i \times F_i - r_{i+1} \times F_{i+1} = [I_i] \ddot{\theta}_i + \dot{\theta}_i \times ([I_i] \dot{\theta}_i) \quad [2]$$

where  $F_i$  and  $F_{i+1}$  are forces acting on link  $i$  at joints  $i$  (distal) and  $i+1$  (proximal), respectively;  $M_i$ ,  $M_{i+1}$  are moments exerted on link  $i$  at joints  $i$  and  $i+1$ , respectively;  $r_i$  and  $r_{i+1}$  are radii from the COM of link  $i$  to the joint centers  $i$  and  $i+1$ , respectively;  $g$  is acceleration due to gravity;  $[I_i]$  is the matrix of inertia; and  $\dot{\theta}_i$  and  $\ddot{\theta}_i$  are vectors of the angular velocity and acceleration for link  $i$ , respectively.

The difference between force and moment values at the point of load application from the estimated inverse dynamics calculations and the directly measured values from the top load cell was considered model error. Force and moment estimations were made with every combination of remaining markers giving a resultant error value for each combination. Errors were calculated for each loading cycle as root mean squared error (RMSE) and normalized RMSE (NRMSE), respectively.

Please see *Appendix II: Manuscript Draft 1* for additional details and figures related to the study methodology.

### Research Accomplishments

#### Specific Aim #1

*MTS testing of running specific prostheses: Completed*  
 The experimental setup was finalized and MTS testing was performed for the existing running-specific prostheses. A representative example of a prosthesis set up in the MTS machine is shown in Figure 2. Reflective markers were placed along the keel of the prosthesis in 2 cm increments and force transducers are present at the base and top of the experimental setup in order to measure forces and moments at the input (top) and “ground” level.



**Figure 2.** Running-specific prosthesis (Ossur Flex-Run) setup in the MTS machine.

#### *Formulating program for data analysis: Completed*

Once raw experimental data were obtained from the MTS testing, we were able to begin formulating the data analysis program in the Matlab programming language and validate the proposed model. Because the project proposed a new model and method to analyze running-specific prostheses, each stage of the program development required validation to ensure proper measurements and calculations. Consequently, this was a lengthy process involving a large amount of troubleshooting. The data analysis program was completed so the results could be used to validate the marker model. Please see the data generated from this programming in the *Reportable Outcomes* section of this document.

#### *Validation of model: Completed*

The programming and model validation were completed for use in the analysis of the MTS data to determine the final marker model.

#### *Analysis of MTS data to determine model: Completed*

Determining the final marker model for each specific prosthesis design was completed. Completion of this task was delayed beyond the originally proposed timeline due to procurement issues with the prosthetic companies. These issues were resolved and the task was completed. This task completes the goals set for Specific Aim 1.

### Specific Aim #2

#### *Determine model with optimal marker placement for all prosthesis designs: Completed*

This task was proposed for Months 13-18 of the project and required the completion of tasks in Specific Aim 1. This task was delayed due to prosthesis procurement issues. However, the task was completed as proposed.

### Results

Data are presented for anteroposterior (AP) force, vertical force, and flexion moment values throughout the cyclical loading task. Figure 3 compares the directly measured values with those estimated from thousands of different combinations of marker placements on the prosthesis. Figure 4 displays the raw error between the estimated force and moment values and the directly measured values for each of the marker placement combinations. Figure 5 shows the NRMSE, representing the difference (in percent) between the directly measured (via load cell) and estimated (via inverse dynamics) proximal forces and moments calculated for each marker combinations.

The Freedom Innovations Nitro prosthesis had a maximal RMSE range of 0.26 N (AP force), 4.45 N (vertical force), and 1.02 Nm (flexion moment) and a maximal NRMSE range of 0.02%, 0.17%, and 0.86% for AP force, vertical force, and flexion moment, respectively across all stiffness categories and all tested combinations of markers. The Ossur Flex-Run prosthesis had a maximal RMSE range of 4.37 N (AP force), 5.88 N (vertical force), and 1.05 Nm (flexion moment) and a maximal NRMSE range of 0.37%, 0.28%, and 0.56% for AP force, vertical force, and flexion moment, respectively across all stiffness categories and all tested combinations of markers. The Ossur Cheetah prosthesis had a maximal RMSE range of 0.99 N (AP force), 9.38 N (vertical force), and 0.73 Nm (flexion moment) and a maximal NRMSE range of 0.12%, 0.44%, and 0.53% for AP force, vertical force, and flexion moment, respectively across all stiffness categories and all tested combinations of markers. The Ottobock 1E90 prosthesis had a maximal RMSE range of 0.48 N (AP force), 7.54 N (vertical force), and 0.54 Nm (flexion

moment) and a maximal NRMSE range of 0.07%, 0.35%, and 0.31% for AP force, vertical force, and flexion moment, respectively across all stiffness categories and all tested combinations of markers.

Figures 6-8 show the average RMSE values for AP force, vertical force, and flexion moment, respectively, for each prosthesis across the number of markers on the prosthesis. All tested combinations with the number of markers indicated were averaged to generate each data point.

Cumulatively, these data indicate little difference in kinetic calculations between the directly measured values and any marker placement or combination of markers. Consequently, a single marker can be placed on any point of a running-specific prosthesis to achieve accurate proximal kinetic estimations.

Please see *Appendix II: Manuscript Draft 1* for a more detailed report of the study results.

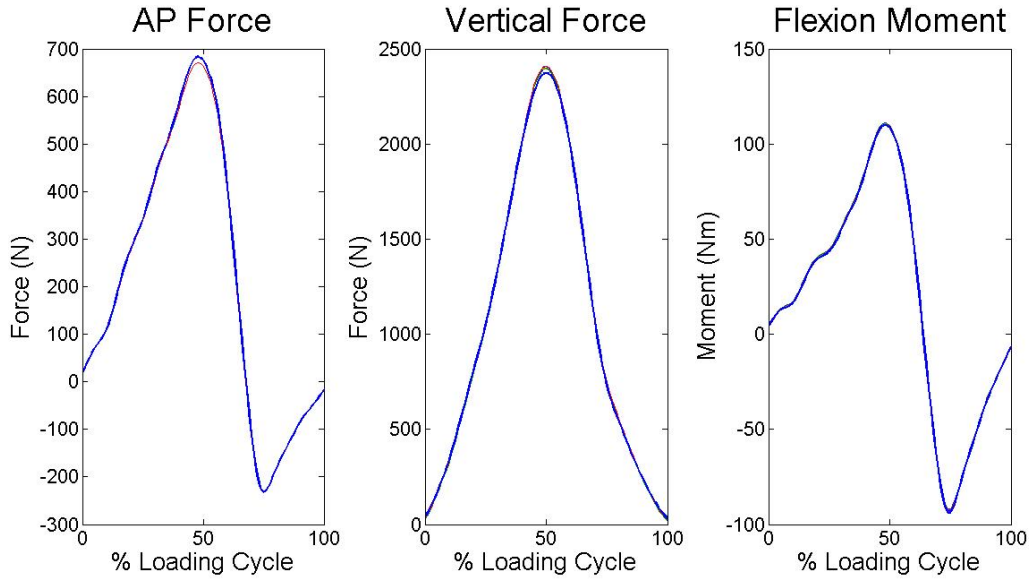


**Figure 3.** AP force, vertical force, and flexion moment curves for cyclical loading. Thick blue lines represent the directly measured values from the upper load cell. Thin lines represent calculated values from each different combination of markers. Exemplar data is from the Ossur Flex Run category 3 prosthesis. Other tested prostheses and stiffness categories showed similar results.

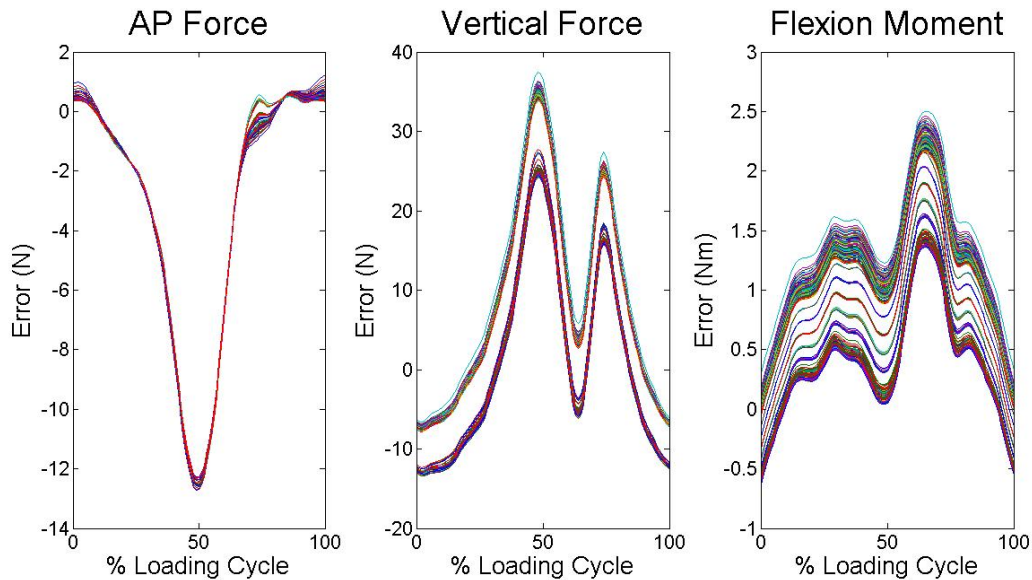


**Figure 4.** Average AP force, vertical force, and flexion moment error curves for the loading cycle. Each curve represents the difference between the directly measured values from the upper load cell and calculated values from each combination of markers on the prosthesis. Exemplar data is from the Ossur Flex Run category 3 prosthesis. Other tested prostheses and stiffness categories showed similar results.

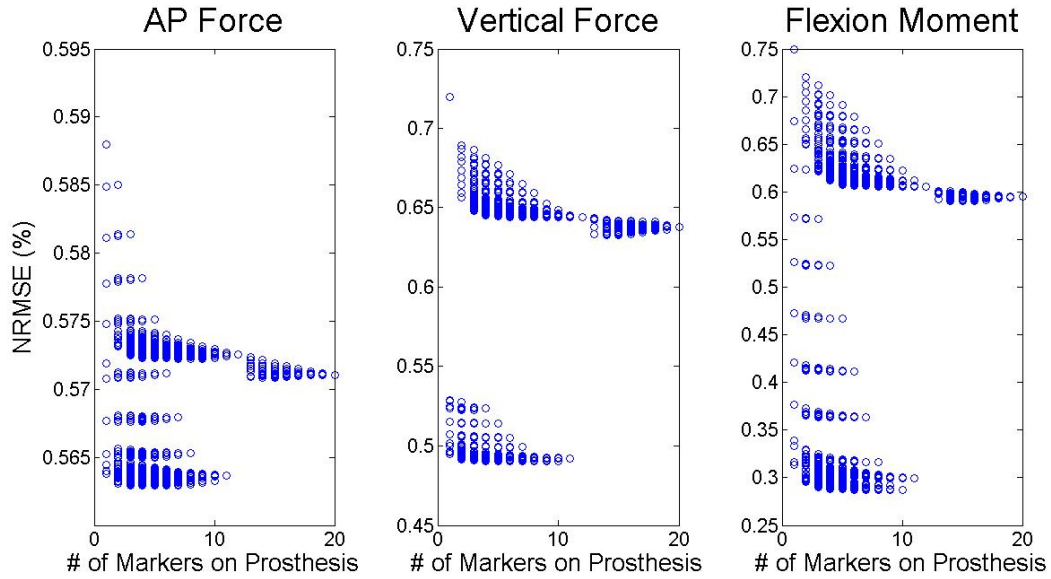


**Figure 5.** Normalized root mean square error (NRMSE) for each combination of markers for AP force, vertical force, and flexion moments throughout the loading cycle. Each dot represents the NRMSE value for a particular combination of markers. The x-axis shows the number of markers on the prosthesis for the particular combination. Exemplar data is from the Ossur Flex Run category 3 prosthesis. Other tested prostheses and stiffness categories showed similar results.

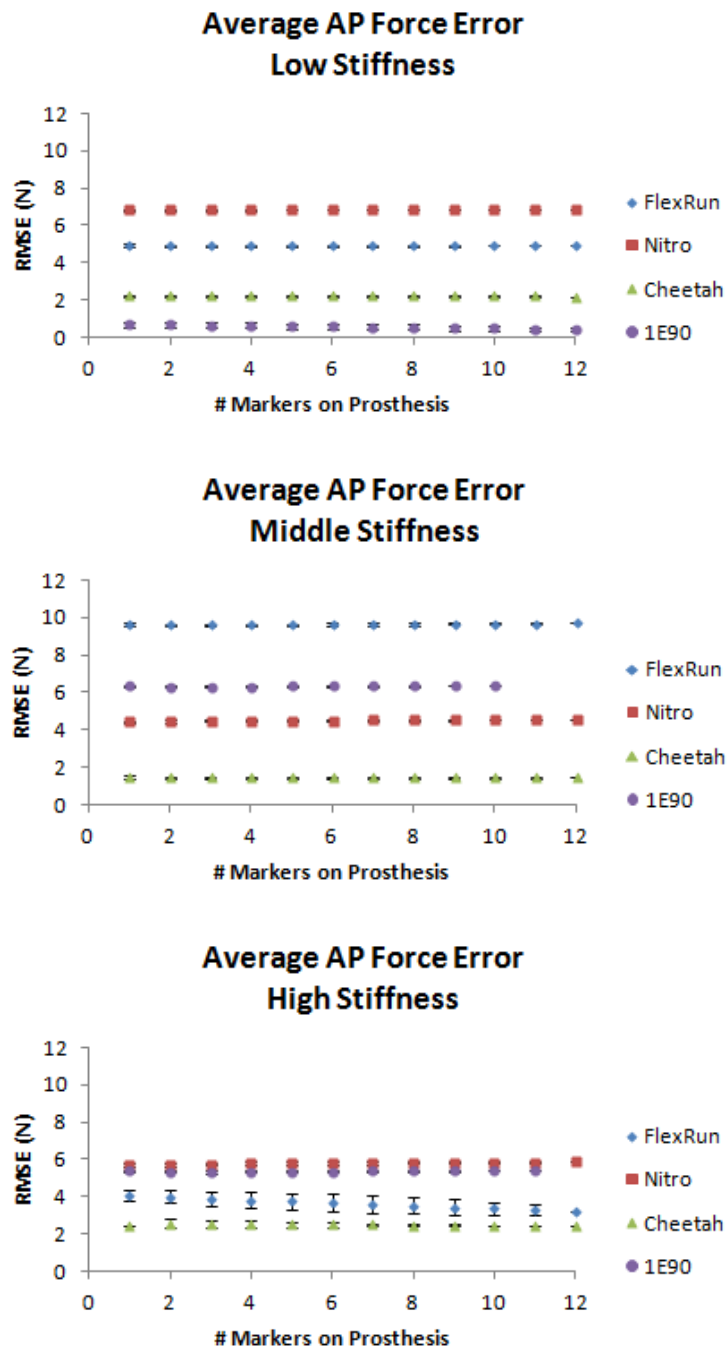


**Figure 6.** Average anteroposterior (AP) force root mean squared error (RMSE) for each prosthesis across the number of markers on the prosthesis. All tested combinations with the number of markers indicated were averaged to generate each data point. Error bars represent  $\pm 1$  standard deviation of all marker combinations tested for the number of markers shown.

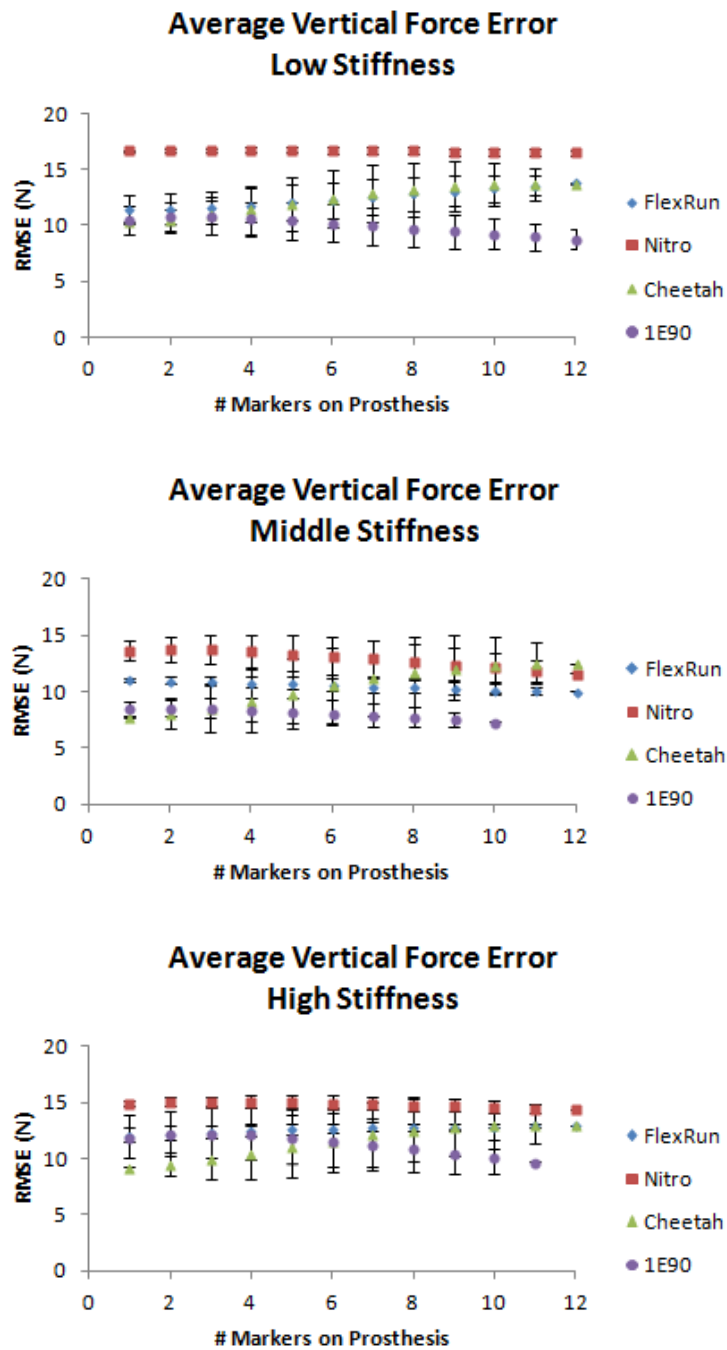
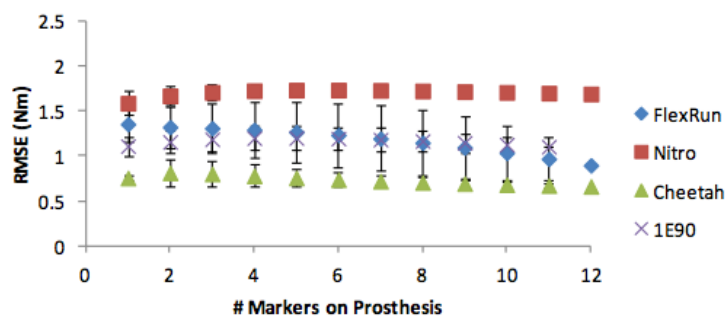
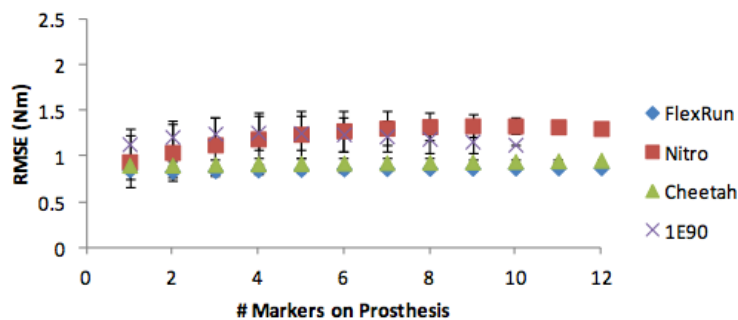


**Figure 7.** Average vertical force root mean squared error (RMSE) for each prosthesis across the number of markers on the prosthesis. All tested combinations with the number of markers indicated were averaged to generate each data point. Error bars represent  $\pm 1$  standard deviation of all marker combinations tested for the number of markers shown.

### Average Flexion Moment RMSE Greatest Stiffness Category



### Average Flexion Moment RMSE Middle Stiffness Category



### Average Flexion Moment RMSE Lowest Stiffness Category

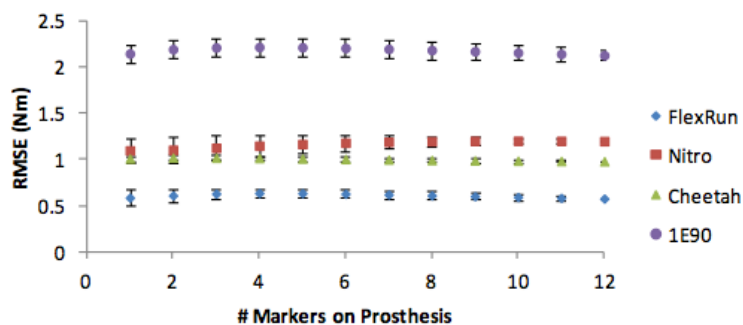


**Figure 8.** Average flexion moment root mean squared error (RMSE) for each prosthesis across the number of markers on the prosthesis. All tested combinations with the number of markers indicated were averaged to generate each data point. Error bars represent  $\pm 1$  standard deviation of all marker combinations tested for the number of markers shown.

## Key Research Accomplishments

- Experimental setup and testing protocol were completed.
- Formulation of the program for data analysis was completed.
- Validation of the program and model was completed.
- Determining the final marker model for each specific prosthesis design was completed.
- Determining a resultant marker model for all tested running prosthesis designs was completed.
- **This research determined that neither the number of markers placed nor the placement of the markers on a running-specific prosthesis influence the force and torque transfer estimations to the proximal end of the prosthesis during stance phase.**
- A manuscript for journal publication is currently in review. A draft of this manuscript is included as *Appendix II: Manuscript Draft 1* of this document.

## Reportable Outcomes

### Manuscripts Supported by this Award

1. Baum BS, Koh K, Linberg A, Tian A, Kim H, Hsieh A, Wolf EJ, Shim JK. (In Review). *Marker placement on running-specific prostheses does not affect kinetics*. Journal of Biomechanics.
2. Baum BS, Schultz MP, Tian A, Shefter B, Shim JK. (In Preparation). *Determining the inertial properties of running-specific prostheses*. Archives of Physical Medicine and Rehabilitation.

### Meeting Abstracts Supported by this Award

1. Baum BS, Shim JK. (2009) *Optimization and validation of a biomechanical model for running-specific prostheses*. Research Interaction Day, University of Maryland, College Park (September 18, College Park, MD).
2. Baum BS, Borjian R, Kim YS, Linberg A, Shim JK. (2010) *Optimization and validation of a biomechanical model for analyzing running-specific prostheses*. The 26<sup>th</sup> Southern Biomedical Engineering Conference (April 30-May 2, College Park, MD).
3. Baum BS, Borjian R, Linberg A, Koh K, Shim JK. (2011) *Optimization and validation of a biomechanical model for running-specific prostheses*. The 15th Annual Meeting of the Gait and Clinical Movement Analysis Society (April 26-29, Bethesda, MD).

### Funding Applied for Based on Work Supported by this Award

1. Shim JK (PI), Baum BS (AI, Project Coordinator), *A New Biomechanical Model to Examine Joint Control Adaptations during Running in Individuals with Lower Extremity Amputation*, National Institute of Arthritis and Musculoskeletal and Skin Disease (NIAMS) R03 Award,

### Degrees Obtained Based on Work Supported by this Award

1. Brian S. Baum, Doctor of Philosophy degree, Anticipated March 2012. Dissertation: *Kinetics in Individuals with Unilateral Transtibial Amputations using Running-Specific Prostheses*.

## Conclusions

The research project has been completed as proposed and a manuscript with the final data is in review. Some unexpected difficulties (e.g. procurement of prostheses; detailed in the August 2010 Annual Report for this project ) delayed portions of the research in the first year of the project. A no-cost extension was granted based on these issues. The issues were resolved and did not affect the overall successful completion of the project.

The data shown in the Body section allowed us to identify the iterations (combinations of marker placements) that yielded acceptable error between the estimated (via inverse dynamics calculations) and directly measured (via load cell) force and moment values. These data indicate that marker placements on running-specific prostheses can be flexible if only kinetic analyses are desired; however, more specific marker placements are recommended if kinematic information about the prosthesis compression is of interest. These data will guide future research and provide greater confidence in reported kinetic results in the past literature.

The data indicate that the marker combinations tested result in errors of less than 1.9% for force and moment calculations for all running prosthesis designs. These data suggest that placing one marker on a running-specific prosthesis is sufficient for accurate joint kinetic analyses for the proximal joints during stance phase of running. Additional research investigating stance phase joint kinetics during amputee running may now be conducted with the knowledge that marker placement does not greatly influence these outcome measures.

This knowledge also allows a larger number of research laboratories to perform running analyses since fewer motion capture cameras would be needed to perform the analysis. This will also dramatically reduce the setup time (fewer markers = less time spent during setup) and the impact on the individual being tested.

Please see *Appendix II: Manuscript Draft 1* for a more detailed report of the study conclusions.

The current study used geometric estimations to predict the inertial properties of the prosthesis subsegments. The inertial properties of different running-specific prosthesis models has not been reported in the literature, yet these data are necessary as inputs to the inverse dynamics equations of motion. Additional research is warranted to accurately determine these inertial parameters of running-specific prostheses to be used in conjunction with the marker placement data reported in the current study for the analysis of overground running kinetics in the amputee population. As an extension of the current study, we performed inertial testing of the running-specific prostheses and a draft of a manuscript resulting from this work is included as *Appendix II: Manuscript Draft 2*. These data will provide researchers with guidelines to assist with determining the inertial properties of running-specific prostheses or with estimations to use in their own analyses if they cannot perform inertial testing at their facilities.

## References

1. Buckley JG. Sprint kinematics of athletes with lower-limb amputations. *Arch Phys Med Rehabil* 1999;80(5):501-8.
2. Buckley JG. Biomechanical adaptations of transtibial amputee sprinting in athletes using dedicated prostheses. *Clinical biomechanics (Bristol, Avon)* 2000;15(5):352-8.
3. Burkett B, Smeathers J, Barker T. Walking and running inter-limb asymmetry for Paralympic trans-femoral amputees, a biomechanical analysis. *Prosthet Orthot Int* 2003;27(1):36-47.
4. Goujon H, Bonnet X, Sautreuil P, Maurisset M, Darmon L, Fode P et al. A functional evaluation of prosthetic foot kinematics during lower-limb amputee gait. *Prosthetics and Orthotics International* 2006;30(2):213-23.
5. Silverman AK, Fey NP, Portillo A, Walden JG, Bosker G, Neptune RR. Compensatory mechanisms in below-knee amputee gait in response to increasing steady-state walking speeds. *Gait & posture* 2008;28:602-9.
6. Selles RW, Bussmann JB, Klip LM, Speet B, Van Soest AJ, Stam HJ. Adaptations to mass perturbations in transtibial amputees: Kinetic or kinematic invariance? *Archives of physical medicine and rehabilitation* 2004;85(12):2046-52.
7. Winter DA, Sienko SE. Biomechanics of below-knee amputee gait. *J Biomech* 1988;21(5):361-7.
8. Sanderson D, Martin P. Joint kinetics in unilateral below-knee amputee patients during running. *Archives of Physical Medicine and Rehabilitation* 1996;77:1279.
9. Buckley J. Sprint kinematics of athletes with lower-limb amputations. *Archives of Physical Medicine and Rehabilitation* 1999;80:501-8.
10. Buckley JG. Biomechanical adaptations of transtibial amputee sprinting in athletes using dedicated prostheses. *Clinical Biomechanics* 2000;15:352-8.
11. Burkett B, Smeathers J, Barker T. Walking and running inter-limb asymmetry for Paralympic trans-femoral amputees, a biomechanical analysis. *Prosthetics and Orthotics International* 2003;27:36-47.
12. Lechler K. Lower-limb prosthetics – Design improvements of a prosthetic spring foot. *Proceedings of the Journal Proceedings of the American Academy of Orthotics and Prosthetics*; 2005.
13. Nolan L. Carbon fibre prostheses and running in amputees: A review. *Foot and Ankle Surgery* 2008;14:125-9.
14. Gailey R. Optimizing prosthetic running performance of the transtibial amputee. *Proceedings of the Proceedings of the AOPA Annual Meeting*; 2003.
15. Hafner BJ, Sanders JE, Czerniecki JM, Ferguson J. Transtibial energy-storage-and-return prosthetic devices: a review of energy concepts and a proposed nomenclature. *J Rehabil Res Dev* 2002;39(1):1-11.
16. Grabowski AM, McGowan CP, McDermott WJ, Beale MT, Kram R, Herr HM. Running-specific prostheses limit ground-force during sprinting. *Biology Letters* 2010;6:201-4.
17. Ferris DP, Louie M, Farley CT. Running in the real world : adjusting leg stiffness for different surfaces. *Proceedings, Biological Sciences* 1998;265(1400):989-94.
18. Weyand PG, Sternlight DB, Bellizzi MJ, Wright S. Faster top running speeds are achieved with greater ground forces not more rapid leg movements. *Journal of applied physiology (Bethesda, Md : 1985)* 2000;89(5):1991-9.

19. Zatsiorsky VM. Kinetics of Human Motion. Champaign, IL: Human Kinetics; 2002.
20. Norvell DC, Czerniecki JM, Reiber GE, Maynard C, Pecoraro JA, Weiss NS. The prevalence of knee pain and symptomatic knee osteoarthritis among veteran traumatic amputees and nonamputees. *Arch Phys Med Rehabil* 2005;86(3):487-93.
21. Andriacchi TP, Mündermann A. The role of ambulatory mechanics in the initiation and progression of knee osteoarthritis. *Curr Opin Rheumatol* 2006;18(5):514-8.
22. Andriacchi TP, Koo S, Scanlan SF. Gait mechanics influence healthy cartilage morphology and osteoarthritis of the knee. *J Bone Joint Surg Am* 2009;91 Suppl 1:95-101.

## **Appendix I. Personnel Receiving Pay**

The following individuals received pay as a part of this grant:

1. Jae Kun Shim, PhD (PI)
2. Adam Hsieh, PhD (Co-PI)
3. Roozbeh Borjian, MS (Technician)
4. Prabhav Saraswat, PhD (postdoc)

**Marker Placement on Running-Specific Prostheses Does Not Affect Kinetics**

**Abstract**

Gait analyses for individuals wearing running-specific prostheses (RSPs) are currently performed by placing reflective markers arbitrarily on the RSP and inverse dynamics techniques are then used to estimate joint kinetic data. Marker placements on RSPs have not been validated for accuracy in estimating joint kinetic data and potential errors within these estimations are unknown. This study examined how varying marker placements on RSPs affect proximal kinetic estimations during an axial loading task. Reflective markers were placed every 2 cm along the lateral aspects of four RSP models with three different stiffness categories each (12 total RSPs). Prostheses were neutrally aligned in a material testing system (MTS) between two load cells that measured proximal applied forces and moments and distal ground reaction forces. RSPs were axially loaded to 2500N of force to simulate peak running loads. Inverse dynamics estimated force transfers from the ground to the proximal endpoint of the prostheses through the segments defined by reflective markers. Errors between estimated and applied values at the proximal endpoint were calculated for every combination of markers. Regardless of the number of markers or their placement on the RSPs, joint kinetic estimations resulted in root mean square errors less than 10 N (1%), 17.5 N (0.75%), and 2.5 Nm (1.6%) for AP force, vertical force, and flexion moment, respectively as compared to the directly measured values at the proximal end of the prostheses. The results suggest that placing a single marker on an RSP is sufficient for accurate stance phase kinetic analyses.

## Introduction

During three-dimensional gait analyses, reflective markers are placed on anatomical landmarks to estimate the positions of joint centers and to define the body segment motions. The distal joint motion data along with ground reaction force data from a force platform can be used as inputs to inverse dynamics equations to estimate proximal joint kinetic values. In locomotion studies using prostheses, markers defining the most distal joint axis, usually the ankle, are generally affixed to spots on the prosthetic foot that mimic the relative marker location on the intact foot and ankle complex<sup>1-6</sup>. Prostheses are often modeled anthropometrically like an intact limb even though these devices may not have the same architecture or landmarks<sup>7-9</sup>.

With the development of running-specific prostheses (RSPs), new prosthetic foot designs have emerged that no longer resemble the human foot. Many of the designs resemble a “C” or “L” shape at the distal end of the limb, which allows the prosthesis to flex and return more energy for propulsion during running, similar to a spring. Placing multiple markers to model RSPs as multisegmented objects during amputee locomotion studies provides a great challenge since definitive joint axes may not exist within the prosthetic foot design, yet modeling RSPs as single rigid objects may not be appropriate since these devices are designed to flex throughout their length. In the face of these challenges, many researchers analyze these prostheses using similar biomechanical analysis methods as have been employed in prosthetic feet designed for walking and intact feet. Studies investigating running with RSPs have estimated the prosthetic limb “ankle” joint to be either at the same relative position as the intact limb’s ankle joint (Figure 1a) or the most acute point on the prosthesis curvature (i.e., the greatest curvature; Figure 1b)<sup>6, 10</sup>,

\*\*\* INSERT FIGURE 1 ABOUT HERE \*\*\*

These estimations have not been validated and potentially result in significant errors within the kinetic calculations and subsequent interpretations of results. Using the intact limb as a reference for marker placement also excludes such a model from use on individuals with bilateral amputations. Consequently, researchers need to know how marker placement on RSPs affects proximal joint kinetic estimations so models can be created for use with different RSP designs and can be utilized in individuals with bilateral lower extremity amputations. An accurate model will provide data that can be interpreted with confidence and is needed to produce biomechanical and physiological data necessary to identify optimal running techniques, prosthetic alignment, prosthetic designs, training regimens, and energy efficiency.

In addition to the different designs of running-specific prostheses, each of these devices are manufactured in different stiffness categories that are generally prescribed based on an individual's body weight and general activity level. A heavier person is typically prescribed a RSP with a higher category of stiffness (higher categories correspond to greater prosthesis stiffness). Studies investigating prosthesis stiffness indicate that the stiffness affects performance, so body weight and general activity level may be insufficient guidelines for prescribing a stiffness category. A stiffer forefoot, wider c-curve, and thinner lay-up resulted in individuals with lower extremity amputation (ILEA) running their fastest sprint times<sup>12</sup>, which suggests that sprint speed can be a function of stiffness and prosthetic foot shape<sup>13</sup>. Using a greater category of stiffness may also improve gait symmetry values for ILEA with transtibial amputation<sup>14, 15</sup>, but it has also been shown to reduce energy efficiency<sup>16</sup>. These data suggest that different prosthesis stiffness categories could affect the performance of the prosthesis and therefore the force and moment transfer through the device.

The aim of this study was to investigate the effect of marker placement on errors between calculated force and moment values from inverse dynamics estimations and directly measured values for specific running prosthesis designs and stiffness categories. We hypothesized that more markers placed on any running-specific prosthesis with any stiffness category would result in the least error in proximal force and moment estimations.

## **Methods**

Four of the most commonly prescribed running-specific prostheses currently available on the market were tested including the 1E90 Sprinter (OttoBock Inc.), Flex-Run (Ossur), Cheetah (Ossur) and Nitro Running Foot (Freedom Innovations) (Figure 2). Three different stiffness categories were also tested for each prosthetic design to identify whether prosthetic stiffness affects marker placement results. Stiffness categories, presented in Table 1, were chosen to reflect a common range of stiffnesses that might be prescribed. OttoBock does not use the term “category” to reflect stiffness, rather different prosthesis stiffnesses are reflected by the target weight of the person using the device. Prostheses were aligned neutrally according to manufacturer recommendations with their proximal ends attached to a six-degree-of-freedom load cell (Bertec PY6, Columbus, OH) that was connected to the arm of a material testing system (MTS, Eden Prairie, MN). A second load cell was secured to the base of the MTS (Figure 3). The prostheses were cyclically loaded for ten cycles with axial forces up to 2,500 N to simulate peak vertical forces commonly observed during running<sup>17-19</sup> (approximately three times the body weight of a 75 kg person). The load cells sampled data at 1000 Hz and measured the forces and moments at the point of load application proximal to the prostheses (applied load) and the reaction forces distal to the prostheses (ground reaction forces).

\*\*\* INSERT TABLE 1 ABOUT HERE \*\*\*

\*\*\*INSERT FIGURE 2 ABOUT HERE \*\*\*

Reflective markers were placed at 2 cm intervals along the lateral aspect of the keel of each running-specific prosthesis (see Figure 3). Reflective markers were also placed orthogonally on the anterior, lateral, and medial aspect of the “head” of the prosthesis, at the point of connection to the socket or pylon, in order to define the local coordinate system of the prosthesis. Three additional markers were placed along the midline of each prosthesis to define a plane to which the keel markers were projected for further analysis. An 8-camera motion capture system (Vicon, Oxford, UK) with a capture frequency of 500 Hz was used to collect the 3-D positional data of the markers during each trial. Two consecutive projected midline markers defined individual segments of the prosthesis (assumed to be rigid) and consecutive segments shared a common marker. The joint between these segments was assumed as a hinge joint. Standard inverse dynamics calculations<sup>20</sup> were made to estimate the force and torque transfer from the ground reaction force, through the defined prosthesis segments, and to the point of load application proximal to the prosthesis.

\*\*\* INSERT FIGURE 3 ABOUT HERE \*\*\*

\*\*\* INSERT FIGURE 4 ABOUT HERE \*\*\*

Prosthesis thickness was measured at each marker position using digital calipers, and prosthesis width at each position was calculated as twice the distance between the marker and its midline projection. Prosthesis segments were defined by two consecutive markers and were considered as rigid trapezoidal cuboids (see Figure 4). The center of mass along the width and thickness of each segment were determined from half the average width and thickness, respectively. The center of mass position along the long axis (length) of each segment was determined by equation 1:

$$\frac{w_d + 2w_p}{3(w_p + w_d)} * l \quad [1]$$

where  $w_d$  and  $w_p$  are the distal and proximal end widths and  $l$  is the segment length.

Segment volumes were estimated as a trapezoidal cuboid volume and the total volume of each prosthesis was estimated by summing all segment volumes. Mass was assumed to be evenly distributed throughout each RSP such that the ratio of segment volume to total volume equaled the ratio of segment mass to total mass, and segment masses were determined accordingly. The inertial properties of each prosthesis segment were estimated using assumptions based on a trapezoidal cuboid. Each segment length was integrated across 200 subsegments. The principal axis moments of inertia of each segment were estimated by equations 2-4:

$$I_{xx} = \sum_1^i [\frac{1}{12} m_i (l_i^2 + w_i^2) + m_i r_i^2] \quad [2]$$

$$I_{yy} = \sum_1^i [\frac{1}{12} m_i (l_i^2 + t_i^2) + m_i r_i^2] \quad [3]$$

$$I_{zz} = \sum_1^i [\frac{1}{12} m_i (w_i^2 + t_i^2)] \quad [4]$$

where  $m_i$  is the mass,  $l_i$  is the length,  $w_i$  is the width,  $t_i$  is the thickness,  $r_i$  is the distance between the subsegment center of mass and the segment center of mass for each subsegment  $i$ , respectively.

The angles between each set of three consecutive markers were calculated throughout the cyclic loading and the range of angle change was determined at each marker “joint”. Markers representing joints that had an angular change of less than one degree were removed from further analyses as they were considered as part of a larger rigid segment. The remaining markers were used for the model analysis. The one degree threshold was determined from the marker position error of the motion capture system.

The difference between force and moment values at the point of load application from the estimated inverse dynamics calculations and the directly measured values from the top load cell was considered model error. Force and moment estimations were made with every combination of remaining markers giving a resultant error value for each combination. Error was calculated for each loading cycle using equations 5 and 6 for root mean squared error (RMSE) and normalized RMSE (NRMSE), respectively.

$$RMSE = \frac{\sum (K_m - K_c)^2}{n} \quad [5]$$

$$NRMSE = \frac{RMSE}{(K_{mmax} - K_{min})} \% \quad [6]$$

where  $K_m$  represents the directly measured kinetic values (force or moment) from the upper load cell,  $K_c$  represents the calculated kinetic values from inverse dynamics equations,  $n$  is the number of data points in the loading cycle, and  $max$  and  $min$  represent the maximum and minimum values within the loading cycle, respectively.

### *Uncertainty Analysis*

The effects of input variable uncertainties were used to estimate the uncertainty of the resultant joint force and moment variables via an error analysis method. The upper bound of uncertainty in the result  $u_R$  was calculated according to equation 7:<sup>21, 22</sup>

$$u_R = \pm \sqrt{\sum_{i=1}^n \left( \frac{\partial R}{\partial x_i} \Delta x_i \right)^2} \quad [7]$$

where  $R$  is the resultant value (e.g. joint force or joint moment),  $x_i$  is the  $i^{\text{th}}$  input variable in predicting  $R$ , and  $\Delta x_i$  is the error associated with input variable  $x_i$ . Primary sources of error ( $\Delta x_i$ ) included errors related to load cell measurements and marker noise which affects segmental kinematic parameters. The uncertainties estimated for AP force, vertical force, and flexion moment for each prosthesis are shown in Table 2.

\*\*\* INSERT TABLE 2 ABOUT HERE \*\*\*

## Results

Calculated values and error data are presented for anteroposterior (AP) forces, vertical forces, and flexion moments during the cyclical loading trials for each prosthesis. Mediolateral (ML) forces, ML rotational moments, and internal/external rotational moments are not presented since the axial loading of the prostheses produced minimal forces and moments along and about these axes, respectively.

Regardless of the number of markers or their placement on the various RSPs, force and moment calculations using inverse dynamics techniques resulted in errors of less than 1.6% as compared to the directly measured values (Table 3). Directly measured and calculated AP force, vertical force, and flexion moment values are presented in Figure 5. Raw errors between the directly measured and calculated forces and moments are presented in Figure 6.

\*\*\* INSERT TABLE 3 ABOUT HERE \*\*\*

\*\*\* INSERT FIGURE 5 ABOUT HERE \*\*\*

\*\*\* INSERT FIGURE 6 ABOUT HERE \*\*\*

The Freedom Innovations Nitro prosthesis had a maximal RMSE range of 0.26 N (AP force), 4.45 N (vertical force), and 1.02 Nm (flexion moment) and a maximal NRMSE range of 0.02%, 0.17%, and 0.86% for AP force, vertical force, and flexion moment, respectively across all stiffness categories and all tested combinations of markers. The Ossur Flex-Run prosthesis had a maximal RMSE range of 4.37 N (AP force), 5.88 N (vertical force), and 1.05 Nm (flexion moment) and a maximal NRMSE range of 0.37%, 0.28%, and 0.56% for AP force, vertical force, and flexion moment, respectively across all stiffness categories and all tested combinations of

markers. The Ossur Cheetah prosthesis had a maximal RMSE range of 0.99 N (AP force), 9.38 N (vertical force), and 0.73 Nm (flexion moment) and a maximal NRMSE range of 0.12%, 0.44%, and 0.53% for AP force, vertical force, and flexion moment, respectively across all stiffness categories and all tested combinations of markers. The Ottobock 1E90 prosthesis had a maximal RMSE range of 0.48 N (AP force), 7.54 N (vertical force), and 0.54 Nm (flexion moment) and a maximal NRMSE range of 0.07%, 0.35%, and 0.31% for AP force, vertical force, and flexion moment, respectively across all stiffness categories and all tested combinations of markers.

The average AP force, vertical force, and flexion moment RMSE values for each combination according to the number of markers on the prostheses are shown in Figure 7. These data show little difference in RMSE values in kinetic variables regardless of the number of markers on a prosthesis.

\*\*\* INSERT FIGURE 7 ABOUT HERE \*\*\*

## **Discussion**

This study examined the effects of marker placement on proximal kinetic estimations using inverse dynamics during a cyclic loading task with running-specific prostheses. The results of this study indicated that root mean square errors between the directly measured and calculated kinetic variables were less than 18N for vertical forces, 10N for AP forces, and 2Nm for flexion moments. Considering peak values of approximately 2500N, 700N, and 120Nm for vertical force, AP force, and flexion moment, respectively, NRMSE values were less than or equal to 1.6% for all combinations of marker placements across all prostheses investigated. These low errors indicate that using any combination of markers would result in proximal joint kinetic estimations with reasonable errors for a gait analysis.

To investigate whether placing a particular number of markers on a prosthesis would have an effect on the outcome variables, the average RMSE values were calculated for all combinations of a particular number of markers. For example, errors were averaged for all combinations of one marker placed on a prosthesis, all combinations of two markers placed on a prosthesis, all combinations of three markers placed on a prosthesis, etc. This data showed similar average RMSE values for the combinations of particular numbers of markers placed on the prostheses (see Figure 7). This information combined with the relatively small range of errors across all tested marker combinations suggest that the number and placement of markers on any of the tested running-specific prostheses does not greatly influence the estimation of force and moment transfer through the prostheses. The estimated uncertainty values for AP force, vertical force, and flexion moment were less than 1% of the peak force and moment values. The range of RMSE across marker combinations for any prosthesis was similar to the uncertainty values for that prosthesis indicating that all marker combinations had similar RMSE values.

One possible explanation for the small change in error across different marker positions is that the magnitudes of the ground reaction forces during running are very large in comparison to the accelerations and inertial properties of the running-specific prostheses. During force transfer from the ground through the prostheses, the centers of mass of the prosthesis subsegments do not change dramatically (low accelerations). Therefore, the ground reaction force transfers nearly unattenuated through the prosthesis. The ground reaction forces also generate torques that account for nearly all of the estimated proximal joint moments while the moments of inertia and the angular velocities of the prosthetic segments contribute relatively little to stance phase kinetics.

These data suggest that kinetic data calculated from prior research with RSPs may be interpreted with greater confidence. Placing markers at the same relative position as the intact limb's ankle joint or the most acute point on the prosthesis curvature<sup>6, 10, 11</sup> should yield similar results in resultant kinetic values proximal to the prosthesis. However, for consistency and flexibility in modeling, it is recommended that markers are placed according to the prosthesis architecture rather than intact limb architecture. This will allow markers to be placed on the same location of a particular prosthesis from subject to subject and will allow for the study of ILEA with bilateral amputations and comparison of these individuals with those with unilateral amputations.

Most motion capture laboratories have a limited number of cameras and may have difficulty tracking a large number of markers placed closely together during activities such as running. This limits the number of markers that researchers can feasibly place on the keel of a running-specific prosthesis, especially considering that the thin profile of such prostheses often necessitates using markers with small diameters. Furthermore, motion capture of overground running requires a large capture volume, and optimizing camera placement for large volumes reduces the effectiveness of these systems to capture small markers in close proximity to each other. Utilizing a minimal marker set for running-specific prostheses will enable widespread use of such a model regardless of the number of cameras available to a laboratory and to allow for both overground and treadmill data collections while using the same model. Additionally, fewer markers on a prosthesis makes setup less tedious and saves testing time.

Several limitations exist in this study. First, only axial loading was performed on the prostheses, whereas when running, the prostheses are loaded while rolling forward, which would produce different loading patterns and potentially different prosthetic bending. This could affect

the recommended marker placements on the prostheses. However, the overall ground reaction forces during running are still much larger than the inertial properties of the prostheses, so it is anticipated that for kinetic analyses, the results presented in this study would generalize to overground running. However, due to the axial loading, this study only presented AP force, vertical force, and flexion moment results. Validation of the marker models is still needed for mediolateral forces, varus/valgus moments, and internal/external rotational moments. Additional studies are warranted to investigate these kinetic parameters using either a 6-degree-of-freedom material testing system that could mimic the prosthetic roll-over during running or direct load measurements at the proximal end of the prosthesis during running. An additional limitation of this study is that only stance phase loading was investigated. The inertial effects of the running prostheses during swing phase are most likely not trivial, so accurate measures of mass, center of mass position, and moments of inertia are needed to accurately estimate the joint kinetic values proximal to the prostheses. Future studies are needed to accurately measure and predict the inertial properties and effects of running-specific prostheses during the running swing phase.

The development and validation of an accurate biomechanical model for use with running-specific prostheses allows researchers to fully examine the kinematic and kinetic adaptations that occur during running in ILEA. Extremely limited information is available in the literature to guide clinicians in aligning, prescribing, or rehabilitating ILEA who wish to run. For example, it is currently unknown whether running with running-specific prostheses poses an increased risk for injury in the residual limb joints or joints in the contralateral limb. ILEA are already at greater risk of degenerative joint diseases such as osteoarthritis (OA)<sup>23</sup>, and the larger forces generated during running could promote the development and progression of these diseases. Prior research supports that OA may initiate in joints that experience a traumatic or

chronic event (such as amputation due to injury or disease) that causes kinematic changes<sup>24</sup>. The rate of OA progression is currently thought to be associated with increased loads during ambulation<sup>24, 25</sup>. Identifying running techniques, prosthetic alignments, or new prosthetic designs that reduce peak lower extremity joint loading may reduce the risk of developing and progressing OA.

Additional research needs include investigating the effects of various prosthetic components in meeting different running goals, and determining optimal prosthetic alignment so as to minimize asymmetries and maximize energy efficiency during running.

## **Conclusions**

Regardless of the number of markers or their placement on the various RSPs, joint kinetic estimations resulted in root mean square errors less than 10 N (1%), 17.5 N (0.75%), and 2.5 Nm (1.6%) for AP force, vertical force, and flexion moment, respectively as compared to the directly measured values at the proximal end of the prostheses during axial loading up to 2,500 N. This affords researchers the flexibility to place markers conveniently on running-specific prostheses and still confidently estimate joint kinetic data during the stance phase of running.

## **Acknowledgements**

This work was funded by the DOD Deployment Related Medical Research Program Grant #W81XWH-09-2-0067.

## References

1. Goujon H, Bonnet X, Sautreuil P, Maurisset M, Darmon L, Fode P et al. A functional evaluation of prosthetic foot kinematics during lower-limb amputee gait. *Prosthetics and Orthotics International* 2006;30(2):213-23.
2. Silverman AK, Fey NP, Portillo A, Walden JG, Bosker G, Neptune RR. Compensatory mechanisms in below-knee amputee gait in response to increasing steady-state walking speeds. *Gait & posture* 2008;28:602-9.
3. Selles RW, Bussmann JB, Klip LM, Speet B, Van Soest AJ, Stam HJ. Adaptations to mass perturbations in transtibial amputees: Kinetic or kinematic invariance? *Archives of physical medicine and rehabilitation* 2004;85(12):2046-52.
4. Winter DA, Sienko SE. Biomechanics of below-knee amputee gait. *J Biomech* 1988;21(5):361-7.
5. Sanderson D, Martin P. Joint kinetics in unilateral below-knee amputee patients during running. *Archives of Physical Medicine and Rehabilitation* 1996;77:1279.
6. Buckley J. Sprint kinematics of athletes with lower-limb amputations. *Archives of Physical Medicine and Rehabilitation* 1999;80:501-8.
7. Royer TD, Wasilewski CA. Hip and knee frontal plane moments in persons with unilateral, trans-tibial amputation. *Gait Posture* 2006;23(3):303-6.
8. Su PF, Gard SA, Lipschutz RD, Kuiken TA. Gait characteristics of persons with bilateral transtibial amputations. *J Rehabil Res Dev* 2007;44(4):491-501.
9. Miller DI. Resultant lower extremity joint moments in below-knee amputees during running stance. *Journal of biomechanics* 1987;20:529-41.

10. Buckley JG. Biomechanical adaptations of transtibial amputee sprinting in athletes using dedicated prostheses. *Clinical Biomechanics* 2000;15:352-8.
11. Burkett B, Smeathers J, Barker T. Walking and running inter-limb asymmetry for Paralympic trans-femoral amputees, a biomechanical analysis. *Prosthetics and Orthotics International* 2003;27:36-47.
12. Lechler K. Lower-limb prosthetics – Design improvements of a prosthetic spring foot. *Proceedings of the Journal Proceedings of the American Academy of Orthotics and Prosthetics*; 2005.
13. Nolan L. Carbon fibre prostheses and running in amputees: A review. *Foot and Ankle Surgery* 2008;14:125-9.
14. Gailey R. Optimizing prosthetic running performance of the transtibial amputee. *Proceedings of the Proceedings of the AOPA Annual Meeting*; 2003.
15. Wilson JR, Asfour S, Abdelrahman KZ, Gailey R. A new methodology to measure the running biomechanics of amputees. *Prosthetics and Orthotics International* 2009;33:218-29.
16. Hafner BJ, Sanders JE, Czerniecki JM, Fergason J. Transtibial energy-storage-and-return prosthetic devices: a review of energy concepts and a proposed nomenclature. *J Rehabil Res Dev* 2002;39(1):1-11.
17. Grabowski AM, McGowan CP, McDermott WJ, Beale MT, Kram R, Herr HM. Running-specific prostheses limit ground-force during sprinting. *Biology Letters* 2010;6:201-4.
18. Ferris DP, Louie M, Farley CT. Running in the real world : adjusting leg stiffness for different surfaces. *Proceedings, Biological Sciences* 1998;265(1400):989-94.

19. Weyand PG, Sternlight DB, Bellizzi MJ, Wright S. Faster top running speeds are achieved with greater ground forces not more rapid leg movements. *Journal of applied physiology* (Bethesda, Md : 1985) 2000;89(5):1991-9.
20. Zatsiorsky VM. *Kinetics of Human Motion*. Champaign, IL: Human Kinetics; 2002.
21. Taylor JR. *An introduction to error analysis : the study of uncertainties in physical measurements*. 2nd ed. Sausalito, Calif.: University Science Books; 1997.
22. Riemer R, Hsiao-Wecksler ET, Zhang X. Uncertainties in inverse dynamics solutions: a comprehensive analysis and an application to gait. *Gait Posture* 2008;27(4):578-88.
23. Norvell DC, Czerniecki JM, Reiber GE, Maynard C, Pecoraro JA, Weiss NS. The prevalence of knee pain and symptomatic knee osteoarthritis among veteran traumatic amputees and nonamputees. *Arch Phys Med Rehabil* 2005;86(3):487-93.
24. Andriacchi TP, Mündermann A. The role of ambulatory mechanics in the initiation and progression of knee osteoarthritis. *Curr Opin Rheumatol* 2006;18(5):514-8.
25. Andriacchi TP, Koo S, Scanlan SF. Gait mechanics influence healthy cartilage morphology and osteoarthritis of the knee. *J Bone Joint Surg Am* 2009;91 Suppl 1:95-101.

## List of Tables

**Table 1.** Stiffness categories used for each prosthesis during testing and the manufacturer recommended body mass range associated with each category.

<b>Prosthesis</b>	<b>Stiffness Category (body mass range)</b>		
Flex-Run	3 (53-59 kg)	5 (69-77 kg)	7 (89-100 kg)
Nitro	3 (60-68 kg)	6 (89-100 kg)	7 (101-116 kg)
Cheetah	3 (60-68 kg)	5 (78-88 kg)	7 (101-116 kg)
1E90	140 lb (63.6 kg)	185 lb (84.1 kg)	235 lb (106.8 kg)

**Table 2.** Uncertainty (U) estimates for each prosthesis when calculating AP force ( $F_x$ ), vertical force ( $F_z$ ) and flexion moment ( $M_y$ ).

<b>Prosthesis</b>	<b>Cat</b>	<b>UF<sub>x</sub> (N)</b>	<b>UF<sub>z</sub> (N)</b>	<b>UM<sub>y</sub> (Nm)</b>
Flex-Run	3	0.232	0.232	0.017
	5	0.441	0.261	0.016
	7	0.168	0.288	0.014
Nitro	3	0.208	0.255	0.030
	6	0.323	0.244	0.022
	7	0.227	0.336	0.019
Cheetah	3	0.225	0.174	0.333
	5	0.300	0.141	0.316
	7	0.384	0.344	0.685
1E90	140lb	0.312	0.198	0.023
	185lb	0.119	0.172	0.043
	235lb	0.129	0.288	0.029

Cat = stiffness category

**Table 3.** Error ranges (minimum to maximum RMSE and NRMSE) of all combinations of markers for the estimated kinetic values from inverse dynamics equations.

		Freedom Innovations			Ossur			Ossur			Ottobock		
		Nitro			Flex-Run			Cheetah			1E90		
Stiffness Category:		Cat 3	Cat 6	Cat 7	Cat 3	Cat 5	Cat 7	Cat 3	Cat 5	Cat 7	140 lb	185 lb	235 lb
AP Force	RMSE (N)	6.78- 6.92	4.32- 4.50	5.66- 5.92	5.17- 9.54	9.39- 9.54	3.23- 4.21	2.17- 2.27	1.36- 1.59	2.46- 3.45	0.29- 0.77	6.27- 6.46	5.28- 5.56
	NRMSE (%)	0.68- 0.69	0.61- 0.63	0.54- 0.56	0.56- 0.93	0.92- 0.93	0.35- 0.45	0.31- 0.32	0.34- 0.40	0.29- 0.41	0.05- 0.12	1.43- 1.47	0.90- 0.95
Vertical Force	RMSE (N)	16.37- 16.80	11.55- 16.00	14.39- 15.85	11.05- 16.93	10.19- 11.95	11.85- 14.18	10.27- 17.41	7.57- 16.95	9.22- 17.49	6.88- 11.93	7.17- 9.61	7.16- 14.70
	NRMSE (%)	0.64- 0.66	0.45- 0.62	0.50- 0.55	0.44- 0.72	0.41- 0.48	0.49- 0.59	0.30- 0.50	0.36- 0.80	0.28- 0.53	0.41- 0.71	0.47- 0.63	0.33- 0.68
Flexion Moment	RMSE (Nm)	0.98- 1.36	0.81- 1.83	1.27- 1.99	0.63- 1.59	0.78- 1.09	0.89- 1.94	0.91- 1.13	0.87- 1.14	0.66- 1.39	2.02- 2.32	0.98- 1.52	1.03- 1.38
	NRMSE (%)	0.52- 0.71	0.67- 1.53	0.72- 1.14	0.31- 0.78	0.37- 0.51	0.48- 1.04	0.67- 0.83	0.53- 0.70	0.46- 0.99	0.75- 0.86	0.58- 0.89	0.38- 0.51

\*Notes: RMSE = root mean square error, NRMSE = normalized root mean square error

## List of Figures

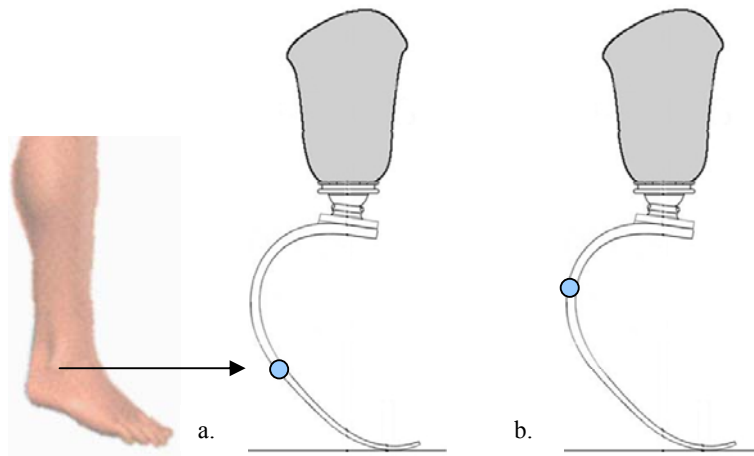


**Figure 1.** Literature has reported marker placement for running prostheses at (a) the height of the intact limb's lateral malleolus or (b) the point at which the radius of the prosthesis is most acute.



a. Freedom Innovations  
Nitro



b. Ossur Flex-Run



c. Ossur Cheetah



d. Ottobock Sprinter  
1E90

**Figure 2.** Prostheses used for mechanical testing.

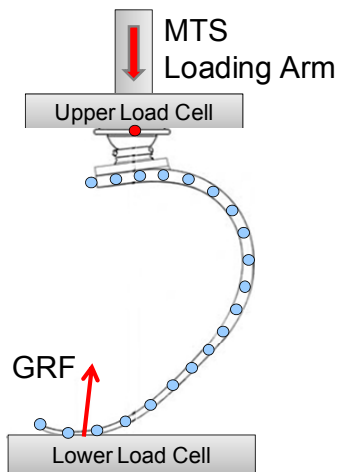


**Figure 3.** Marker placement on a running-specific prosthesis and its position in an MTS machine between two load cells. Fewer markers than actual are shown in the illustration for clarity. The red dot indicates the point of load application, measured by the upper load cell. The lower load cell measured ground reaction force (GRF). The red arrows represent the input and GRF force vectors.

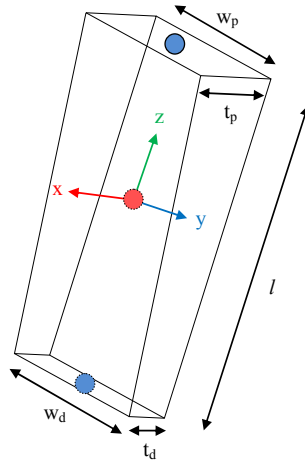


**Figure 4.** Schematic of segment definitions within each prosthesis. Blue circles represent markers, the red circle represents the segment center of mass. The axis defines the segment local coordinate system with its origin at the center of mass. Segment length ( $l$ ) is also shown along with the width ( $w$ ) and thickness ( $t$ ) at the proximal (p) and distal (d) ends.

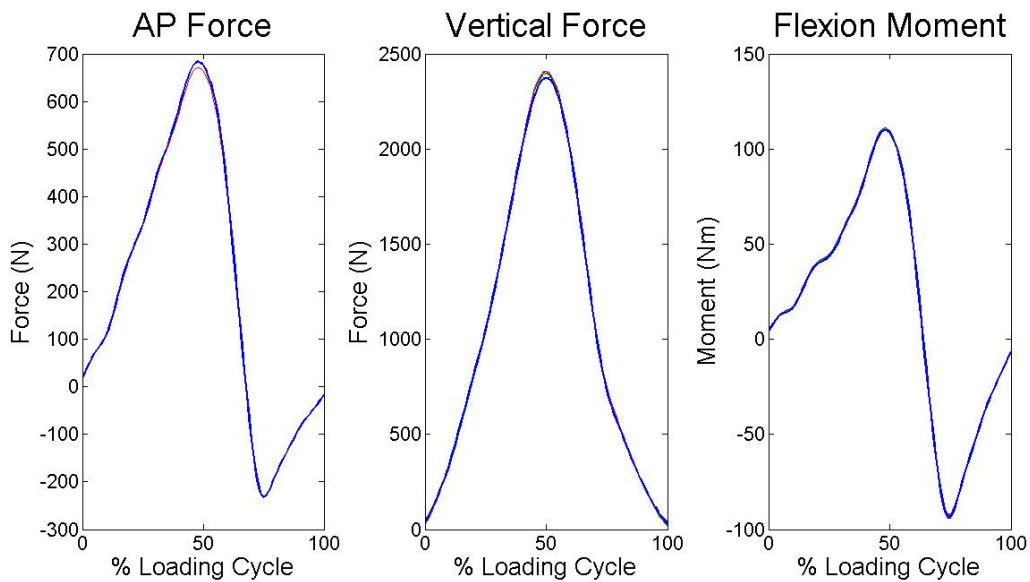


**Figure 5.** Anteroposterior (AP) force, vertical force, and flexion moment curves for cyclical loading. Thick blue lines represent the directly measured values from the upper load cell. Thin lines overlaid on the curves (showing nearly identical patterns) represent calculated values from each different combination of markers. Exemplar data are from the Flex-Run category 3 prosthesis. Other tested prostheses and stiffness categories showed similar results.

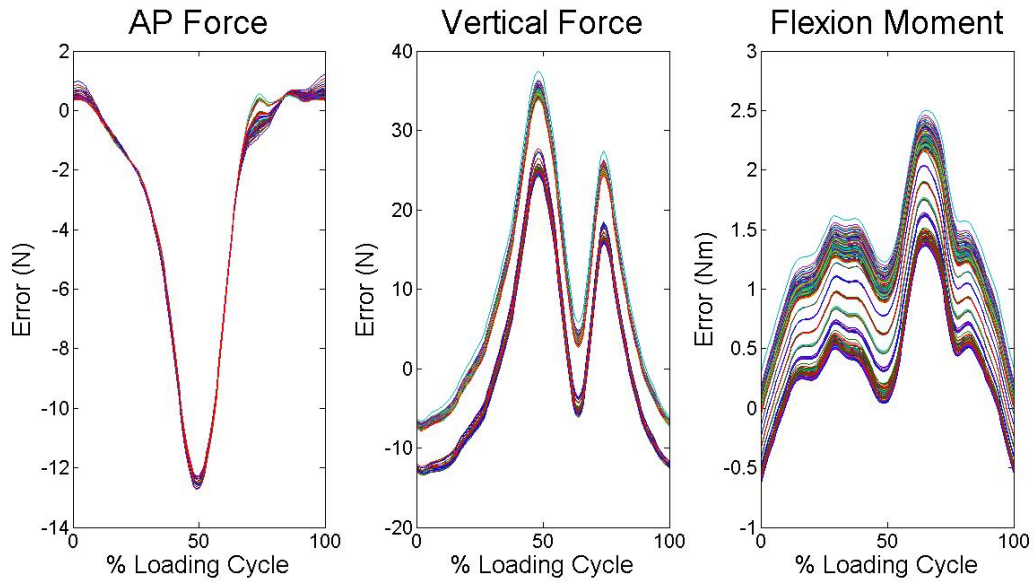


**Figure 6.** Average anteroposterior (AP) force, vertical force, and flexion moment error curves for the loading cycle. Each curve represents the difference between the directly measured values from the upper load cell and calculated values from each combination of markers on the prosthesis. Exemplar data are from the Flex-Run category 3 prosthesis. Other tested prostheses and stiffness categories showed similar results.

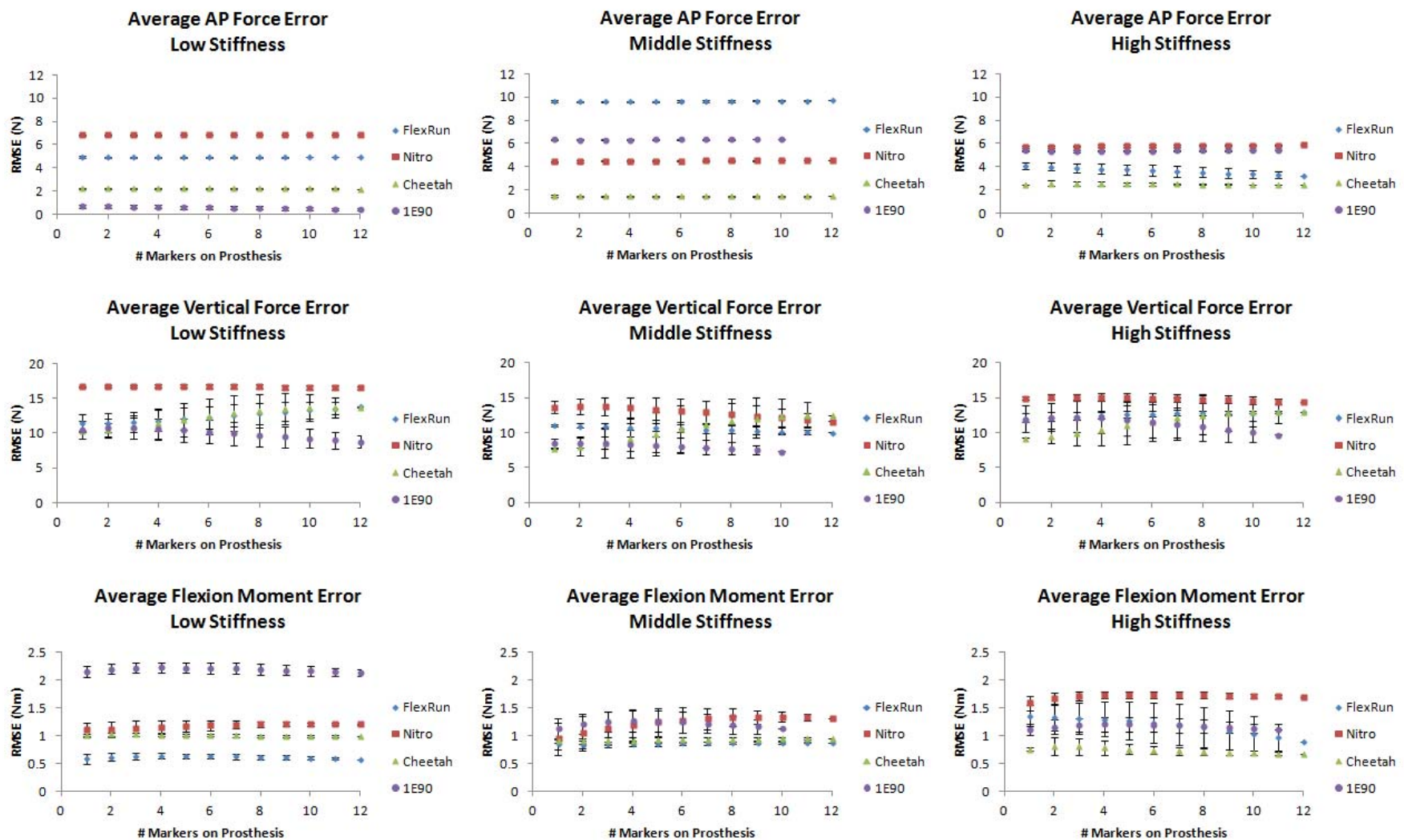


**Figure 7.** Average anteroposterior (AP) force, vertical force, and flexion moment root mean square error (RMSE) for each prosthesis across the number of markers on the prosthesis. All tested combinations with the number of markers indicated were averaged to generate each data point. Error bars represent  $\pm 1$  standard deviation of all marker combinations tested for the number of markers shown.

**Determining the Inertial Properties of Running-Specific Prostheses**

**Abstract**

Body segment inertial properties (mass, center of mass position, and moment of inertia) affect the joint kinetics and subsequent limb control during ambulation. Accurate segment inertial property estimations are necessary for properly calculating kinetic parameters and appropriately interpreting these data. Limited information currently exists related to inertial properties of various running-specific prosthetic designs which limits the joint kinetic information that can be generated and interpreted during running analyses. The purpose of this study was to determine the inertial properties for four of the most common running-specific prostheses currently available on the market across three stiffness categories for each model. A predictive equation was developed to estimate the center of mass (COM) positions of the various prosthetic designs, and a trifilar pendulum is described for measuring the prostheses moments of inertia. The predictive equation matched the measured COM exactly when prosthesis-specific inputs were used and produced errors between 0.1-2.8 cm when using average input values across prostheses for a specific design. The trifilar pendulum estimated inertial properties within  $-6.21 \times 10^{-5} \text{ kg}\cdot\text{m}^2$  ( $\leq 1\%$ ) of a block with known inertia. Misalignments of the block's COM with the pendulum's center of rotation  $\leq 5\text{cm}$  yielded errors  $\leq 0.0027 \text{ kg}\cdot\text{m}^2$ . Inertial properties about any axis varied  $\leq 0.0038 \text{ kg}\cdot\text{m}^2$  within the tested prosthetic designs due to different stiffness categories, although inertial properties differed more substantially between different designs. Inertial estimation errors from pendulum measurements were less than or equal to errors associated with various methods for predicting intact limb inertial properties indicating that the

methods and values presented are within currently accepted tolerances for inertial property estimations for gait studies.

## **Introduction**

Joint kinetic data (e.g. forces, moments, powers, etc.) provide insights into how individuals ambulate and how injured or diseased individuals adapt their joint control to achieve the same movement goals. Link-segment models allow the estimation of proximal joint kinetics from either distal link joint kinetics or from measured distal force data such as ground reaction forces. This is achieved through knowledge of the link motion, inertial properties of link segments, and distal joint kinetic data. Accurate kinetic estimations using link-segment models depend on accurate segment inertial property estimations including mass, center of mass position, and moments of inertia<sup>1</sup>.

Intact limb inertial properties and regression equations have been established through cadaveric studies<sup>2-4</sup> and body scanning methods<sup>5-7</sup>, and are commonly used during gait analyses. However, in individuals with lower extremity amputation (ILEA), prosthetic components replace the intact limbs, and the inertial properties of the resultant limb-prosthesis combination are altered. It is common practice for researchers to approximate the inertial properties of walking prostheses by using the values of intact limbs, since the prostheses assume similar shapes to the foot and have masses comparable to those of the intact limbs. Some researchers suggest that modeling prosthetic feet using the same marker placements and inertial properties as intact limbs produces reasonably acceptable error levels in gait parameters during stance phase<sup>8-10</sup>. However, other research supports the notion that the inertial properties of prosthetic feet significantly impact the resultant joint kinematic and kinetic estimations<sup>11-14</sup> and that more accurate estimations of prosthetic inertial properties are warranted. With the advent of running-specific

prostheses (RSPs), these prosthetic components no longer resemble the intact foot and ankle complex, and they have much smaller masses than the body parts they replace. It is therefore reasonable to assume that RSPs also have substantially different moments of inertia than intact limbs. Currently there is very limited information on the inertial properties of RSPs, measurements of these properties, and the effects that these properties have on joint biomechanics.

To our knowledge, only one study to date<sup>15</sup> has reported any inertial property values for running specific prostheses. This lack of information makes it difficult to compare prosthetic properties between studies and to gain a broader view of population-wide prosthetic inertial parameters. Multiple methods of measuring the inertial properties of objects exist. Genta and Delprete examined these methods and broadly categorized them into oscillatory and acceleratory<sup>16</sup>. They reported that acceleratory methods are more affected by the presence of damping than are oscillatory methods, and that torsional and multifilar pendulums are the most accurate, capable of errors less than 1%. Physical pendulums are most commonly used in the prosthetic literature to measure prosthesis moments of inertia. These pendulums generally rely on a joint or bearing that is assumed to be frictionless to make accurate moment of inertia measurements<sup>17, 18</sup>. In practice, however, friction in this bearing does exist and, along with air resistance, will slow the period of oscillation and impart error in the inertial estimations. One solution to this problem is to perform multiple oscillation trials with the pendulum and use only the first period under the assumption that it best represents the true period of oscillation<sup>17, 19</sup>. An alternative solution is to use other pendulum designs that do not rely on bearings, such as multifilar pendulums. A trifilar pendulum is a form of multifilar pendulum that utilizes a frame or platform suspended from three equidistant wires about which rotation occurs. The wire

suspension virtually eliminates the issues caused by friction from a bearing and allows for accurate measures of an object's moment of inertia about a particular axis of rotation. It also allows for measurements over many more periods of oscillation than physical pendulums.

The purpose of this study was to determine the inertial properties (mass, center of mass, and principal axis moments of inertia) for four of the most common running-specific prostheses (RSPs) currently available on the market. The construction and use of a trifilar pendulum to estimate these values are described in detail. A secondary aim of this project is to determine the error in inertia estimations due to linear and rotational malalignment between an object's (i.e. a RSP) and pendulum's center of mass and axis of rotation, respectively.

## **Methods**

Mass, center of mass positions, and principal axis moments of inertia were estimated from four commonly available running-specific prostheses. The tested models included the Freedom Innovations Nitro, Ossur Cheetah, Ossur Flex-Run, and Otto Bock 1E90. Three different stiffness categories were investigated from each prosthesis model to identify whether inertial differences exist within each model type. Categories are named arbitrarily by the manufacturers, with increasing stiffness correlating with increasing category number. The stiffness categories are typically prescribed according to patient body mass and activity level, with greater categories corresponding to greater weight and activity intensity (i.e. a greater stiffness category would be prescribed for sprinting than for jogging). Stiffness categories are also not standardized across manufacturers, so a comparable range of stiffness categories for each prosthesis was tested. Tested stiffness categories and their corresponding recommended body mass ranges are presented in Table 1.

\*\*\*\*\* INSERT TABLE 1 ABOUT HERE \*\*\*\*\*

### *Mass and Center of Mass*

Prosthesis masses were measured using a standard laboratory scale with a resolution of 1g. The center of mass for each prosthesis in the sagittal plane (x-z plane) was measured using a reaction board method. The mass was assumed to be evenly distributed throughout the frontal plane of the prosthesis such that the local y-coordinate position of the center of mass would be zero for each prosthesis. Based on these data, an equation was developed to estimate the center of mass position for each RSP model relative to the most proximal (“head”) and most distal (“toe”) point on the prosthesis. This equation can be used to estimate the center of mass of a prosthesis in the absence of a reaction board or other equipment needed to directly measure a prosthesis’ center of mass. The center of mass (COM) relates to the head and toe via Equation 1:

$$COM = r|\vec{T}| * \begin{bmatrix} \cos\theta & 0 & \sin\theta \\ 0 & 1 & 0 \\ -\sin\theta & 0 & \cos\theta \end{bmatrix} \begin{bmatrix} u_{Tx} \\ u_{Ty} \\ u_{Tz} \end{bmatrix} \quad [1]$$

where r is the ratio of the head-COM and head-toe vector magnitudes calculated for the different categories,  $|\vec{T}|$  is the magnitude of the head-toe vector,  $\theta$  is the angle between the head-toe and head-COM vectors and is used to define the rotation matrix, and  $u_T$  describes the components (x, y, and z) of the head-toe unit vector. Figure 1 shows a schematic of the relationship between the center of mass, head, and toe of a prosthesis with respect to equation 1.

\*\*\*\*\* INSERT FIGURE 1 ABOUT HERE \*\*\*\*\*

### *Moments of Inertia*

The inertial properties of all prostheses were estimated by placing them on a trifilar pendulum (see Figure 2) and measuring the periods of oscillation, as described by du Bois et al<sup>20</sup>.

The pendulum consisted of an equilateral plexiglass triangle suspended from its corners by equidistant wires. A custom-built aluminum frame served to support the trifilar pendulum. Attention was given to construct equidistant measurements of the pendulum frame and to ensure a level triangular platform. Frame and wire contact points were constructed such as to minimize friction points. A laser sensor (model BJN50-NDT, Autonics, Mundelein, IL; response time < 1ms) measured the pendulum's period of oscillation. The sensor was aligned such that the laser would be interrupted when a corner of the trifilar plate passed the sensor. Two consecutive passes determined one full period of oscillation of the pendulum.

\*\*\*\*\* INSERT FIGURE 2 ABOUT HERE \*\*\*\*\*

The triangular platform's COM was determined as the centroid of the triangle (intersection of the lines formed by the median of each length to the opposing corner). The center of mass in the sagittal plane (the local x-z plane) for each prosthesis was estimated by appropriately orienting and placing the device on a force plate. The resulting center of pressure provided the coordinate of the COM projection onto the force plate. The local x- and z-coordinates relative to the most proximal end of the prosthesis ("head") were then calculated from this projection. The carbon fiber of the prostheses was assumed to have evenly distributed mass, so the y-coordinate of each prosthesis COM was calculated to be aligned with the midline of the prosthesis.

The local coordinate system of each prosthesis was defined to originate at the COM (Figure 3). Each prosthesis design contained a linear "arm" section at its proximal end that was used as a reference to define the primary axes. For the Nitro and Flex-Run models, the most proximal linear segment was horizontal when held in or near a neutral alignment, and was thus used to define the x-axis (antero-posterior). For the Cheetah and 1E90 models, the proximal end

was vertical, and was thus used to define the z-axis (superior-inferior). In all prostheses, the y-axis was parallel to the width of the prosthesis, and orthogonal to the previously defined axis. The final principal axis was defined as orthogonal to both existing axes.

\*\*\*\*\* INSERT FIGURE 3 ABOUT HERE \*\*\*\*\*

\*\*\*\*\* INSERT FIGURE 4 ABOUT HERE \*\*\*\*\*

The principal axis moments of inertia for each prosthesis were estimated by measuring the period of oscillation from the trifilar pendulum. Prostheses were placed on the triangular platform, and the two centers of mass were aligned. In addition, the prosthesis' principal axis was aligned with vertical (Figure 4). The platform-prosthesis system was then oscillated about each primary axis of rotation. The moment of inertia about each axis at the center of mass was calculated via Equation 2<sup>20</sup>.

$$I_{zz} = \frac{R^2 m g \tau^2}{4 \pi^2 L} \quad [2]$$

where  $I_{zz}$  is the moment of inertia about the oscillating axis of the pendulum,  $R$  is the distance from each wire connection to the center of the axis of rotation,  $m$  is the mass of the object,  $g$  is acceleration due to gravity,  $L$  is the length of the wires, and  $\tau$  is the period of oscillation. When adding an object of unknown inertia, the mass and inertia from Equation 2 can be split into components of the frame and object:

$$m = m_P + m_O \quad [3]$$

$$I_{zz} = I_{Pzz} + I_{Ozz} \quad [4]$$

where subscripts  $P$  and  $O$  represent the platform and object, respectively. Therefore, the moment of inertia of the object can be calculated using Equation 5<sup>20</sup>:

$$I_{Ozz} = \frac{R^2 g \tau^2}{4 \pi^2 L} (m_P + m_O) - I_{Pzz} \quad [5]$$

### *System Validation*

To validate the system set-up, a rectangular aluminum block with a known mass (2.45 kg) and known moment of inertia about its horizontal and vertical axes was tested in both positions using the same protocol that was used to test the RSP's. Data was collected, and moments of inertia were calculated and compared to the object's known moments of inertia. System error about each axis of rotation was considered as the difference between the measured and known inertial value about that axis.

Malalignment between the object's and the pendulum's center of mass can introduce error in the moment of inertia estimations as well. Malalignment can either be of a linear nature, i.e. if the object's center of mass is not aligned vertically over the platform's center of mass, or it can be of rotational nature, i.e. the object's principal axis is not vertical. Great care was taken to align the prostheses centers of mass and principal axes with the center of mass and axis of rotation (vertical) of the triangular platform; however, it is possible that these centers of mass and axes were not perfectly aligned. Linear malalignments will cause a shift in the object + platform system's resultant center of mass and the pendulum will no longer oscillate about the intended axis of rotation, thus imparting error in the period and moment of inertia calculations. Rotational malalignments will estimate the moment of inertia about an axis different than the axis of interest. In trifilar pendulums, it is often impossible to ensure exact alignment of the centers of mass and axes of interest of the system, especially when using non-uniformly shaped objects such as prostheses. In order to account for these errors, moment of inertia was measured at varying degrees of both linear and angular malalignment. To test the effects of linear malalignment, the aluminum block, in both the horizontal and vertical positions, was placed 1 cm to 10 cm from the pendulum's axis of rotation at 1cm increments. Moment of inertia was

calculated following the same protocol described earlier and compared to the known moment of inertia of the block about the axis of interest. Mathematically, moment of inertia error due to linear malalignment can be expressed by<sup>20</sup>

$$\varepsilon_D = -\frac{m_Q D^2}{m_P + m_Q} \left( m_P + \frac{m_Q r^2}{4r^2} \right) \quad [6]$$

which is influenced both by the increased inertia of the system (first term) and the change in weight distribution and center of rotation due to the new resultant center of mass position (second term, in parentheses) caused by the malalignment of the plate and object's centers of mass.

\*\*\*\*\* INSERT FIGURE 5 ABOUT HERE \*\*\*\*\*

Rotational malalignment can also affect the accuracy of inertial calculations when oscillating the prosthesis about its principal axes. Each RSP's curved design prevented it from naturally balancing with its principal axes aligned with the pendulum's axis of rotation. To test the effects of rotational malalignment, the middle category of each type of RSP was re-tested with its x- and z-axes tilted  $\pm 5^\circ$  (Figure 5). Moment of inertia was calculated following the same protocol and compared to the moment of inertia of the prosthesis with its principal axes aligned to vertical.

## Results

Each prosthesis' measured and estimated center of mass positions, including the predicted  $r$  and  $\theta$  values are presented in Table 2. Primary axis moments of inertia are presented in Table 3. For all prosthesis designs, the y-axis moment of inertia corresponding to the anatomical flexion/extension axis resulted in the largest moments of inertia whereas the z-axis (anatomical internal/external rotation) had the smallest moments of inertia.

\*\*\*\*\* INSERT TABLE 2 ABOUT HERE \*\*\*\*\*

\*\*\*\*\* INSERT TABLE 3 ABOUT HERE \*\*\*\*\*

System validation with the aluminum block of known moment of inertia showed that the trifilar pendulum was accurate. The error in moment of inertia was  $-6.21 \times 10^{-5} \text{ kg}\cdot\text{m}^2$  for the horizontal and  $-2.65 \times 10^{-6} \text{ kg}\cdot\text{m}^2$  for the vertical position of the aluminum block, which represent a 1% and 0.1% error in the results respectively.

Figure 6 shows errors in moment of inertia due to linear malalignment. Errors are expressed both mathematically (errors in moment of inertia predicted by Equation 6, “calculated”) and as directly measured using the trifilar pendulum (“measured”). The calculated and measured error values show good agreement in linear malalignments less than or equal to five centimeters. Effects of angular malalignment about the x- and z-axes are presented in Table 4.

\*\*\*\*\* INSERT TABLE 4 ABOUT HERE \*\*\*\*\*

\*\*\*\*\* INSERT FIGURE 6 ABOUT HERE \*\*\*\*\*

## **Discussion**

Mass, center of mass positions, and moments of inertia were estimated from three different stiffness categories for each of four different running-specific prosthesis designs. Variations in each of these parameters were identified due to different prosthesis designs and stiffness categories.

The center of mass positions for each prosthesis were calculated using a reaction board, and a predictive equation was developed to estimate these positions using the relationship between the most proximal point, most distal point, and the center of mass position of a

particular prosthetic design. Using the ratio between the head-COM and head-toe vectors along with the angle between these vectors, as illustrated in Table 3, the equation exactly predicted the centers of mass when the category-specific ratio and angles were used. When using the average ratio and angle for each prosthesis, a majority of the centers of mass were predicted to within less than one centimeter of error along the x- and z-axes. Several of the predictions, however, resulted in greater than one centimeter of error with a maximum error of 2.8 centimeters. The larger errors were a result of a greater range of ratio and angle values across the stiffness categories of a particular prosthetic design. Using different body segment parameter models (e.g. cadaveric vs body scanning-based regression equations) to predict the intact foot center of mass position are shown to vary by greater than 2 cm in the predicted positions<sup>21</sup>. This suggests that center of mass predictions within the range reported in this study are reasonable; however, it is recommended that direct measurements of the center of mass position within prostheses be used when possible to ensure the most accurate data and to reduce the possible errors these data will induce in joint kinetic estimations from inverse dynamics equations.

Intact limb inertial property measurements can vary substantially depending on the method used to measure these parameters. Rao et al. (2006) compared segment inertial property estimations using six methodologies including one geometric model, two cadaveric-based models, and three mass scanning models from live subjects.<sup>21</sup> They identified significant differences between methods in all inertial properties for each of the foot, shank, and thigh segments. Estimated moments of inertia for intact limbs are reported to differ by between 0.0025-0.0031 kg·m<sup>2</sup> for the foot, 0.009-0.020 kg·m<sup>2</sup> for the shank, and 0.026-0.085 kg·m<sup>2</sup> for the thigh depending on the calculation method<sup>22, 23</sup>. Moment of inertia estimation errors induced in the current study, by purposely misaligning the aluminum block center of mass with the

pendulum center of mass during oscillation trials, resulted in errors up to  $0.008 \text{ kg}\cdot\text{m}^2$  with a 10cm malalignment (Figure 6). Malalignments of 5cm or less resulted in errors less than  $0.002 \text{ kg}\cdot\text{m}^2$ , which is lower than differences in intact foot moments of inertia due to measurement technique differences. This indicates that using a trifilar pendulum to estimate moments of inertia of prosthetic components will yield errors less than those currently accepted in the literature for intact limbs, as long as the center of mass of the prosthetic device is aligned within 5cm of the pendulum's center of mass. With careful attention, any researcher should be able to reasonably align the centers of mass of a prosthesis and pendulum with errors much smaller than 5cm, which would yield even smaller errors in moment of inertia.

The center of mass and moment of inertia measurements are limited to the prostheses in their uncompressed form (with no load as in swing phase of running). The inertial parameters will change when the prosthesis is compressed (for example, during stance phase of running). However, since the loads required to compress the prosthesis are very large relative to the changes in inertial properties during loading, it is likely that these inertial changes would have a negligible effect on the resultant inverse dynamics estimations of joint kinetic values. Rather the loads (i.e. ground reaction forces) would dominate the inverse dynamics predictions. Additional studies are needed to determine these effects and to discriminate between the effects of inertial changes and the loads required to produce those changes.

## **Conclusions**

The inertial properties of four commonly prescribed running-specific prostheses were measured using a reaction board and a trifilar pendulum. The inertial parameters were shown to vary slightly between stiffness categories within a prosthetic design, and they varied more substantially between different prosthetic designs. A predictive equation was presented to

estimate the center of mass of a prosthesis when direct measurements are not possible. These data may be used for predicting inertial parameters of similar prostheses. The predictive equation and pendulum method presented measured inertial properties with errors equal to or less than those found in commonly used predictive methods for intact limb inertial parameters.

### **Acknowledgements**

This work was funded by the DOD Deployment Related Medical Research Program Grant #W81XWH-09-2-0067 and the University of Maryland Department of Kinesiology Graduate Research Initiative Fund.

## References

1. Winter DA. Biomechanics and motor control of human movement. 3rd ed. Hoboken, N.J.: John Wiley & Sons; 2005.
2. Chandler RF, Clauser CE, McConville JT, Reynolds HM, Young JW. Investigation of the inertial properties of the human body. Ohio: Aerospace Medical Research Laboratories, Wright-Patterson Air Force Base; 1975.
3. Clauser CE, McConville JT, Young JW. Weight, volume and center of mass of segments of the human body. Ohio: Wright-Patterson Air Force Base; 1969.
4. Dempster WT. Space requirements of the seated operator. Ohio: Wright-Patterson Air Force Base; 1955.
5. de Leva P. Adjustments to Zatsiorsky-Seluyanov's segment inertia parameters. *Journal of biomechanics* 1996;29(9):1223-30.
6. Zatsiorsky VM, Seluyanov VN, Chugunova LG. In vivo body segment inertial parameters determination using a gamma-scanner method. In: Berme N, Cappozzo A, editors. *Biomechanics of Human Movement: Applications in Rehabilitation, Sports, and Ergonomics*. Worthington, Ohio: Bertec Corp.; 1990. p 186-202.
7. Zatsiorsky VM, Seluyanov VN, Chugunova LG. Methods of determining mass-inertial characteristics of human body segments. In: Chernyi GG, Regirer SA, editors. *Contemporary Problems of Biomechanics*. Boca Raton, Florida: CRC Press; 1990. p 272-91.
8. Su PF, Gard SA, Lipschutz RD, Kuiken TA. Gait characteristics of persons with bilateral transtibial amputations. *J Rehabil Res Dev* 2007;44(4):491-501.
9. Miller DI. Resultant lower extremity joint moments in below-knee amputees during running stance. *Journal of biomechanics* 1987;20:529-41.

10. Royer TD, Wasilewski CA. Hip and knee frontal plane moments in persons with unilateral, trans-tibial amputation. *Gait Posture* 2006;23(3):303-6.
11. Selles RW, Bussmann JBJ, Wagenaar RC, Stam HJ. Effects of prosthetic mass and mass distribution on kinematics and energetics of prosthetic gait: A systematic review. *Archives of physical medicine and rehabilitation* 1999;80(12):1593-9.
12. Selles RW, Korteland S, Van Soest AJ, Bussmann JB, Stam HJ. Lower-leg inertial properties in transtibial amputees and control subjects and their influence on the swing phase during gait. *Archives of physical medicine and rehabilitation* 2003;84(4):569-77.
13. Selles RW, Bussmann JB, Klip LM, Speet B, Van Soest AJ, Stam HJ. Adaptations to mass perturbations in transtibial amputees: Kinetic or kinematic invariance? *Archives of physical medicine and rehabilitation* 2004;85(12):2046-52.
14. Mattes SJ, Martin PE, Royer TD. Walking symmetry and energy cost in persons with unilateral transtibial amputations: Matching prosthetic and intact limb inertial properties. *Archives of physical medicine and rehabilitation* 2000;81:561-8.
15. Brüggemann G-P, Arampatzis A, Emrich F, Potthast W. Biomechanics of double transtibial amputee sprinting using dedicated sprinting prostheses. *Sports Technology* 2009;1:220-7.
16. Genta G, Delprete C. Some considerations on the experimental determination of moments of inertia. *Meccanica* 1994;29:125-41.
17. Hillery SC, Wallace ES, McIlhagger R, Watson P. The effect of changing the inertia of a trans-tibial dynamic elastic response prosthesis on the kinematics and ground reaction force patterns. *Prosthetics and Orthotics International* 1997;21(2):114-23.

18. Martin PE, Mungiole M, Marzke MW, Longhill JM. The use of magnetic resonance imaging for measuring segment inertial properties. *J Biomech* 1989;22(4):367-76.
19. Smith JD. Effects of prosthesis inertia on the mechanics and energetics of amputee locomotion. The Pennsylvania State University; 2008.
20. du Bois JL, Lieven NaJ, Adhikari S. Error Analysis in Trifilar Inertia Measurements. *Experimental Mechanics* 2008;49(4):533-40.
21. Rao G, Amarantini D, Berton E, Favier D. Influence of body segments' parameters estimation models on inverse dynamics solutions during gait. *Journal of biomechanics* 2006;39(8):1531-6.
22. Goldberg EJ, Requejo PS, Fowler EG. The effect of direct measurement versus cadaver estimates of anthropometry in the calculation of joint moments during above-knee prosthetic gait in pediatrics. *Journal of biomechanics* 2008;41(3):695-700.
23. Kingma I, Toussaint HM, De Looze MP, Van Dieen JH. Segment inertial parameter evaluation in two anthropometric models by application of a dynamic linked segment model. *Journal of Biomechanics* 1996;29(5):693-704.

**List of Table.**

**Table 1.** Stiffness categories used for each prosthesis during testing and the manufacturer recommended body mass range associated with each category.

<b>Prosthesis</b>	<b>Stiffness Category (body mass range)</b>		
Flex-Run	3 (53-59 kg)	5 (69-77 kg)	7 (89-100 kg)
Nitro	3 (60-68 kg)	6 (89-100 kg)	7 (101-116 kg)
Cheetah	3 (60-68 kg)	5 (78-88 kg)	7 (101-116 kg)
1E90	140 lb (63.6 kg)	185 lb (84.1 kg)	235 lb (106.8 kg)

**Table 2.** Center of mass (COM) positions, in m, along the principal axes measured with a reaction board in the sagittal plane (x-z plane) relative to the “head” position (most proximal point on the prosthesis) compared to COM estimated using equation 1 in the text. The y-position of the COM is aligned with the midline of the prosthesis and thus has a zero value. The r and  $\theta$  values specific to each prosthesis exactly predicted the measured COM. The average r and  $\theta$  values measured across stiffness categories for a particular prosthesis design were used as the input variables to predict the estimated COM positions.

Prosthesis	Cat	r	Avg r	$\theta$	Avg $\theta$	Measured COM		Estimated COM		Error	
						x	z	x	z	x	z
<b>Flex-Run</b>	3	0.398		0.951		-0.065	-0.072	-0.069	-0.070	0.004	-0.002
	5	0.418	0.404	1.044	0.999	-0.065	-0.079	-0.059	-0.079	-0.006	0.001
	7	0.395		1.003		-0.058	-0.078	-0.059	-0.080	0.001	0.003
<b>Nitro</b>	3	0.366		1.128		-0.053	-0.069	-0.062	-0.054	0.009	-0.015
	6	0.359	0.362	1.091	1.185	-0.051	-0.069	-0.063	-0.053	0.012	-0.016
	7	0.362		1.336		-0.058	-0.063	-0.054	-0.061	-0.004	-0.002
<b>Cheetah</b>	3	0.504		0.328		0.025	-0.264	0.018	-0.292	0.007	0.028
	5	0.589	0.556	0.377	0.360	0.019	-0.304	0.022	-0.286	-0.003	-0.018
	7	0.574		0.374		0.021	-0.300	0.024	-0.290	-0.003	-0.010
<b>1E90</b>	140lb	0.597		0.441		0.017	-0.307	0.019	-0.286	-0.002	-0.021
	185lb	0.538	0.562	0.452	0.429	0.029	-0.278	0.037	-0.287	-0.008	0.009
	235lb	0.537		0.392		0.032	-0.278	0.023	-0.289	0.009	0.011

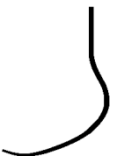
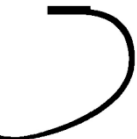
Cat = stiffness category

r = ratio of measured prosthesis head-COM to head-toe vector magnitudes

$\theta$  = angle, in radians, between measured head-COM and head-toe vectors

Error = difference between measured and estimated COM positions, in m

**Table 3.** Mass and moments of inertia calculated about each prosthesis' measured primary axis. Category represents the stiffness category of the prosthesis according to the manufacturer.

Prosthesis Type	Category	Mass (kg)	Moment of Inertia (kg·m <sup>2</sup> )			
			x - axis	y - axis	z - axis	
	Ossur Cheetah	3	0.492	0.0123	0.0139	0.0021
		5	0.511	0.0127	0.0143	0.0023
		7	0.539	0.0136	0.0152	0.0022
	Ossur Flex-Run	3	0.416	0.0037	0.0047	0.0014
		5	0.437	0.0037	0.0051	0.0017
		7	0.466	0.0040	0.0054	0.0017
	Freedom Innovations Nitro	3	0.307	0.0021	0.0029	0.0010
		6	0.349	0.0024	0.0033	0.0012
		7	0.366	0.0026	0.0036	0.0012
	Ottobock 1E90	140lb	0.543	0.0116	0.0130	0.0027
		185lb	0.605	0.0131	0.0152	0.0035
		235lb	0.677	0.0144	0.0168	0.0042

**Table 4.** Error values of angular malalignment of  $\pm 5^\circ$  orientation. Values represent the difference between the prosthesis' measured moment of inertia in neutral alignment and  $\pm 5^\circ$  rotation. Data are presented for the middle stiffness category for each prosthesis.

Prosthesis	x-axis		z-axis	
	-5°	+5°	-5°	+5°
Flex-Run	-0.000009	0.000124	0.000184	0.000138
Nitro	0.000654	0.000707	0.000855	0.000505
Cheetah	-0.000303	0.000765	0.000461	-0.000502
1E90	0.000299	0.001651	0.000755	-0.000750

## List of Figures

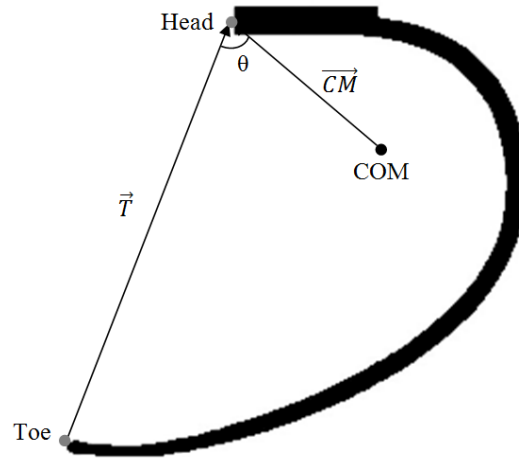


**Figure 1.** Relationship between the center of mass (COM), Head, and Toe of a running-specific prosthesis.  $\vec{T}$  is the Head-Toe vector,  $\overline{CM}$  is the Head-COM vector, and  $\theta$  is the angle between these vectors. Equation 1 in the text may be used to estimate the COM position based on a known  $\theta$  value and ratio between  $\overline{CM}$  and  $\vec{T}$  for a particular running-specific prosthesis design.

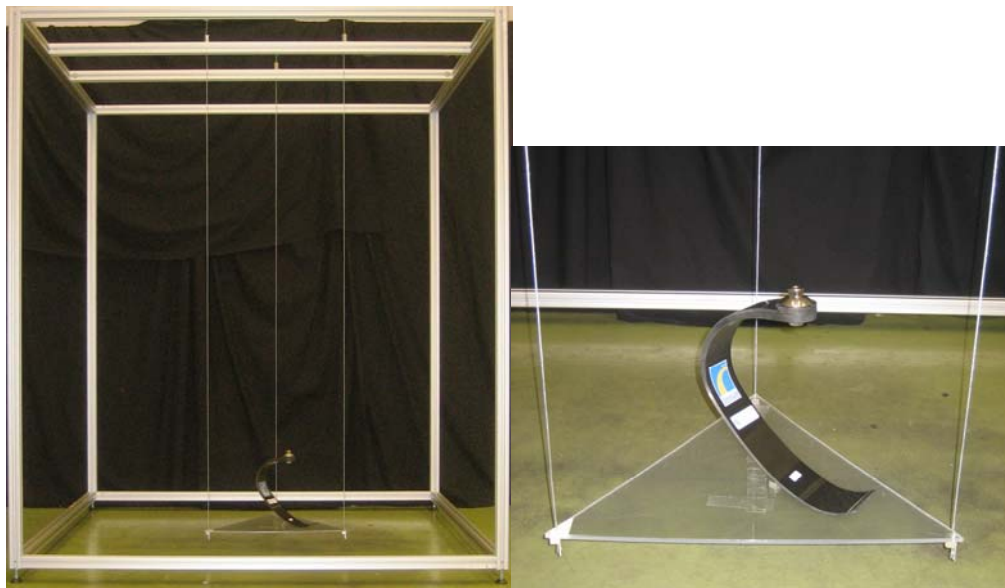
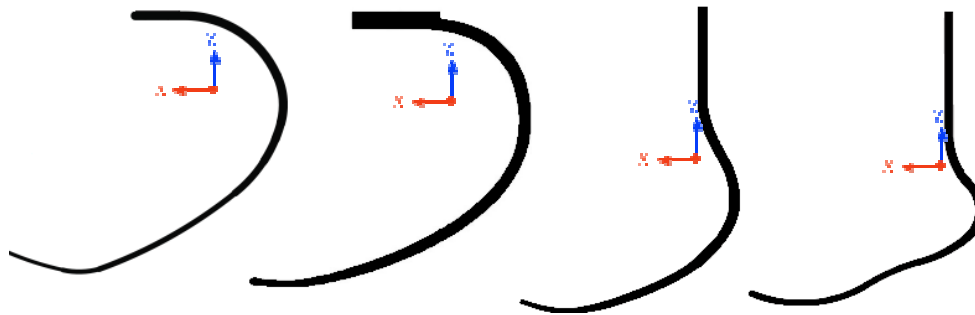


**Figure 2.** Custom-built trifilar pendulum. A triangular platform is suspended from a large frame by three equidistant wires that allow rotation about the platform's center of mass. The moments of inertia of a prosthesis may be calculated directly from the period of oscillation of the pendulum, measured when one corner of the platform passes a laser sensor (not shown).



a. Freedom  
Innovations Nitro

b. Ossur Flex-Run

c. Ossur Cheetah

d. Otto Bock  
Sprinter 1E90

**Figure 3.** The local coordinate systems originating at the centers of mass for each prosthesis. The y-axis is orthogonal to the sagittal plane, with the positive direction pointing at the reader. Details on defining all three axes are included in text.

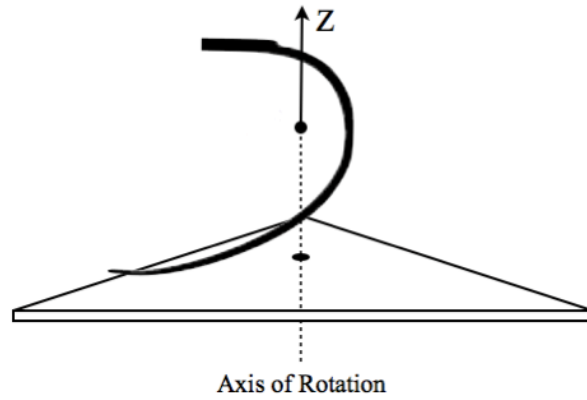


**Figure 4.** Experimental setup. Primary axes of rotation (z-axis shown here) of the prosthesis are aligned with the trifilar pendulum's axis of rotation. The centers of mass of the two systems are aligned.

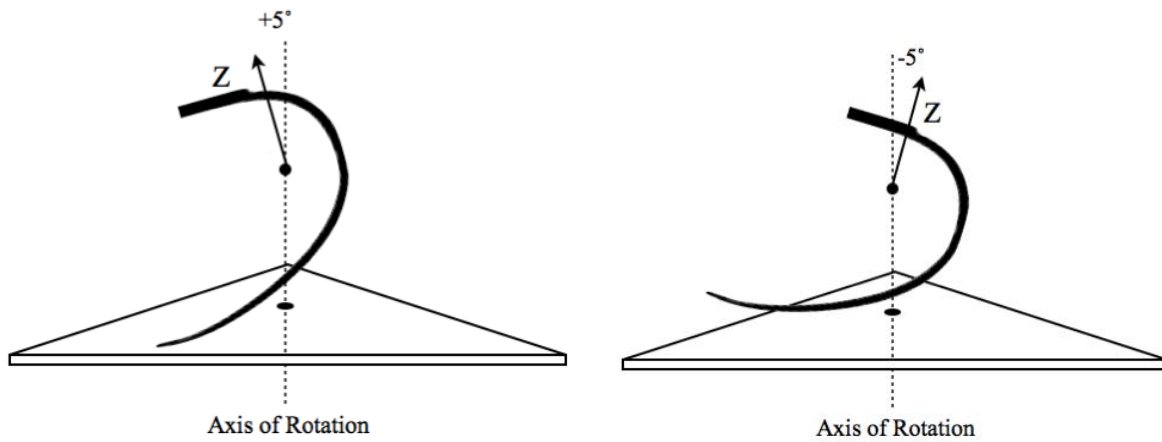


**Figure 5.** Inducing a rotational malalignment of the z-axis for +/-  $5^\circ$  tilt of the intended prosthesis axis of rotation.

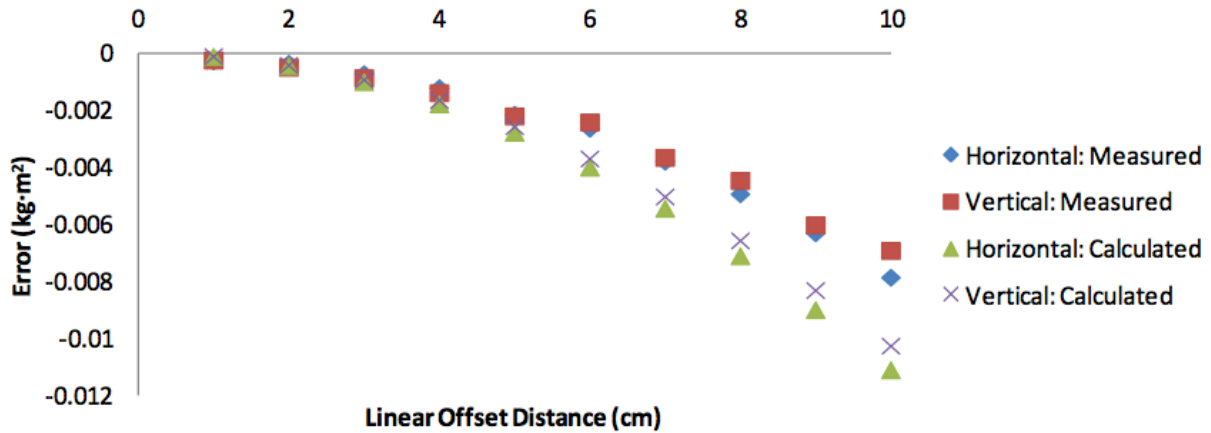


**Figure 6.** Offset error as measured from the linear malalignment testing with the aluminum block and through mathematical calculations. Measured: The block was tested in both the horizontal and vertical position and displaced linearly from the intended axis of rotation in 1 cm increments. Error of MOI is the difference between the known MOI of the block when aligned with the axis of rotation and the measured MOI of the offset block.